Received: 8 March 2021 | Revised: 5 October 2021 | Accepted: 11 January 2022

DOI: 10.1002/fam.3054

RESEARCH ARTICLE

WILEY

Reconstruction of the Grenfell Tower fire—Part 5: Contribution to the understanding of the tenability conditions inside the apartments following the façade fire

Eric Guillaume[1] | Virginie Dréan[1] | Bertrand Girardin[1] | Talal Fateh[2,3]

[1]Efectis France, Saint Aubin Cedex, France

[2]Efectis UK-Ireland, Newtownabbey, UK

[3]Ulster University, FIRESERT, Newtownabbey, UK

Correspondence
Eric Guillaume, Efectis France, route de l'Orme des Merisiers, 91193 Saint Aubin Cedex, France.
Email: eric.guillaume@efectis.com

Summary

The serious fire incident at Grenfell Tower in London, involving a combustible façade system that was installed as part of a major refurbishment of the building, has raised concerns regarding the fire risk that these systems pose. The fire spread over the façade of the Tower was previously numerically modelled and this model was validated by comparison with observational data. This model was used to determine the fire behavior of the façade and the fire's propagation into apartments through windows. In the present paper, impact models are used to evaluate tenability conditions inside the Tower, especially for the apartments in the first corner of the Tower that caught fire. The source of toxic effluents includes the components used in the refurbishment of the façade and the apartment furniture. Different hypotheses of gas yields are tested to assess variability and unknowns in the burning conditions. An extensive literature review was conducted to investigate the toxic yields to be considered in the simulations. Tenability conditions are assessed for each apartment during the fire spread over the façade. This leads to the quantification of the thermal and toxic environment inside the apartments. Two different models are tested for thermal and toxic threats, and the influence of the insulation material used in the façade is investigated. The results showed that the same conclusion can be made regardless of the input data for toxicity and the model used, within the limits of the studied dataset and conditions. Fires from the apartments quickly drive tenability conditions, independently of the dataset and model used, and even if mineral wool is used instead of poly-isocyanurate as façade insulant.

KEYWORDS

CFD, façade insulation, fire propagation, impact model, ISO 13571, numerical simulation, toxicity, ventilated façade

1 | INTRODUCTION

The Grenfell Tower is a 24-storey high-rise building located in London. It was refurbished in the period 2012-2016 with a new insulated ventilated façade system and new windows installed on all of the building's elevations. The Grenfell Tower tragedy happened on 14 June 2017.[1] The fire spread to the façade via external flaming from an apartment located on a lower residential floor of the east face of

the Tower. This has been extensively detailed in expert reports[2–5] and in video and photographic records of the real fire. These records were used to provide an analysis of the post-break-out vertical and horizontal fire propagation over the whole façade of the Grenfell Tower in reference 6.

The performance of the façade system installed on the Grenfell Tower was simulated using a model that was validated at intermediate and large scales, as addressed in references 7,8.The simulations closely matched the experimental results of reference 9 and confirmed that the aluminum composite material (ACM) cladding was the main element driving the global fire behaviour of the tested façade systems. In particular, systems that featured ACM cladding made with a polyethylene core (ACM-PE) showed extensive fire propagation regardless of the insulant used.[8,12]

The fire development inside the initial apartment of Grenfell Tower and its behaviour at the kitchen window was investigated numerically in reference 10. The overall heat release rate (HRR) for typical apartment rooms and window failure criteria were estimated roughly, based on assumed apartment contents prior to the fire. A complementary thermomechanical analysis of window failure was performed previously and reported in reference 11.

The full height of the Grenfell façade was modelled numerically using the computational fluid dynamics (CFD) code fire dynamics simulator (FDS)[14–17] to determine its fire behaviour.[12,13] The vertical and horizontal fire spread over the façade of the Tower were validated by comparison with video and photographic observations of the real fire. The numerically predicted fire propagation was consistent with observations of the disaster.[6]

The Tower perimeter included a series of 14 columns: five columns on the north and south faces of the building leading to four bays, and four columns for the east and west faces of the building, leading to three bays. Hence, respectively, the north and south faces, and the east and west faces were identical. From levels 4 to 23, all floors had a similar layout of six flats (four two-bedroom flats and two one-bedroom flats) and a lobby. These flats are called "X1" to "X6" in this paper. For example, "X6" flats referred to the apartments from 16 (4th floor) to 206 (23th floor), and "X1" flats referred to the apartments from 11 (4th floor) to 201 (23th floor).

Observations from the fire, detailed in reports[2–5] and in reference 6, have shown that the spread of fire over the Tower can be split into different periods. During the period from 01:08 a.m. to 01:29 a.m., approximately, external flames spread over the east face of the Tower. Occupants of flats with windows located on that side of the Tower corresponding to the "X6" flats position (from flat 16 to flat 206, Figure 9), were the first that have seen flames close to their windows, followed by smoke and flames entering their flats. The abbreviation of the "X1" to "X6" localization is reminded in Figure 1. The fire originated in "X1" at the fourth level of the Tower. Occupants evacuated, and no fatalities were observed in "X6" flats.[3,5] After this period, dense irritant smoke started to accumulate in the burning "X6" flats, and spread out from the main doors of flats because of their poor fire performance, into common lobbies and into the stairs. This gradually prevented evacuation from flats to flats either on the same floor or to lower floors by the stair, while these other apartments were affected by increasing toxic smoke from the outside façade fire and from the smoke in the lobbies.

After 01:29 a.m. during the Grenfell disaster, when the fire had reached the top of the Tower, observations showed that strongly enhanced horizontal fire propagation occurred, especially via the Tower's architectural crown. The fire spreads across the four faces of the Tower from 01:29 up to 04:09 a.m., due to the combustion of the insulated façade system and the apartment contents. As the fire spread over the façade, window failures led to more and more fires developing in flats. The fire propagation from the façade into the apartments through windows was previously assessed numerically and validated by comparison with observations.[12,13]

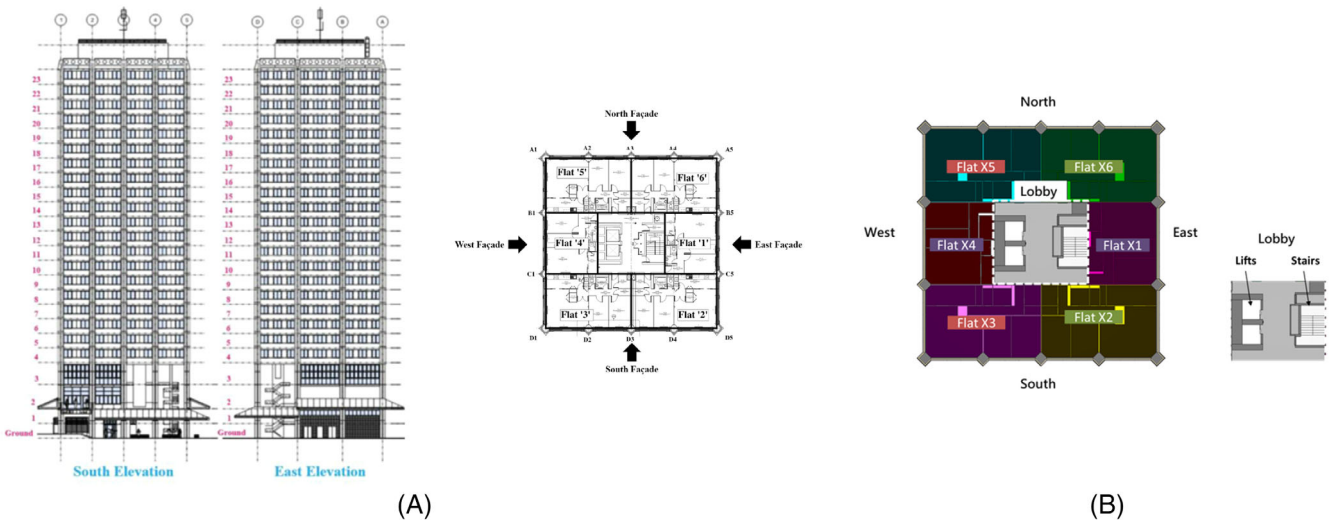

FIGURE 1 (A) Original schematic representation of floor plan for the 4 to 23th floors of Grenfell Tower[3]; (B) Abbreviation of the flat localization used in the numerical model

The current paper presents an impact model that considers fire loads from the façade system and from apartment furniture. Tenability conditions are assessed in terms of thermal effects and toxicity[34–37] during the fire spread over the façade of the Tower. This allows the quantification of the conditions inside the Tower and an analysis of the contribution of the façade and other building fabric components, and that of the apartments' contents.

Existing methods often consider only smoke density and/or carbon monoxide, with yields often treated as constants, usually assuming a well-ventilated fire. This is the case for the CFD code FDS[14–17] used in this study, where the effluent yields are constant for a given combustion reaction, and will not depend on the ventilation conditions. An extensive bibliographic study was conducted to investigate toxic and asphyxiant effluent yields, mainly CO and HCN, to be used in simulations. The objective was to reproduce, in the simulations, the change in CO and HCN yields depending on the fire development. In the simulations, a change in the effluent released from the fire is assumed in the toxicity analysis, taking into consideration ventilation conditions. The different scenarios considered are detailed in Section 4.4. The yields were evaluated for several test methods and ventilation conditions. Furthermore, two revisions of the International Standard are addressed to evaluate their difference on the model impact results assessed.

This publication does not assess tenability conditions for individual occupants, for two reasons. First, such analysis requests a lot of behavioral and movement data that are not necessarily available and may be highly speculative, reducing the validity of the analysis. Second, individual cases are ethically difficult to analyze in such a recent fire with many fatalities and an inquiry still undergoing. So, only general tenability conditions per room are presented hereafter. In this research, individual situations are not addressed. The work presented is very sensitive to the assumptions made, and it is our decision not to extrapolate to individual cases.

2 | SMOKE TOXICITY AND GRENFELL FIRE

A global synthesis of the previous research and main findings from Grenfell incident reconstruction is addressed in Figure 2. This multi-step research was performed with highly interdependent parts, both experimental and numerical. The synoptic allows the understanding of the whole approach from the very first step of this research.

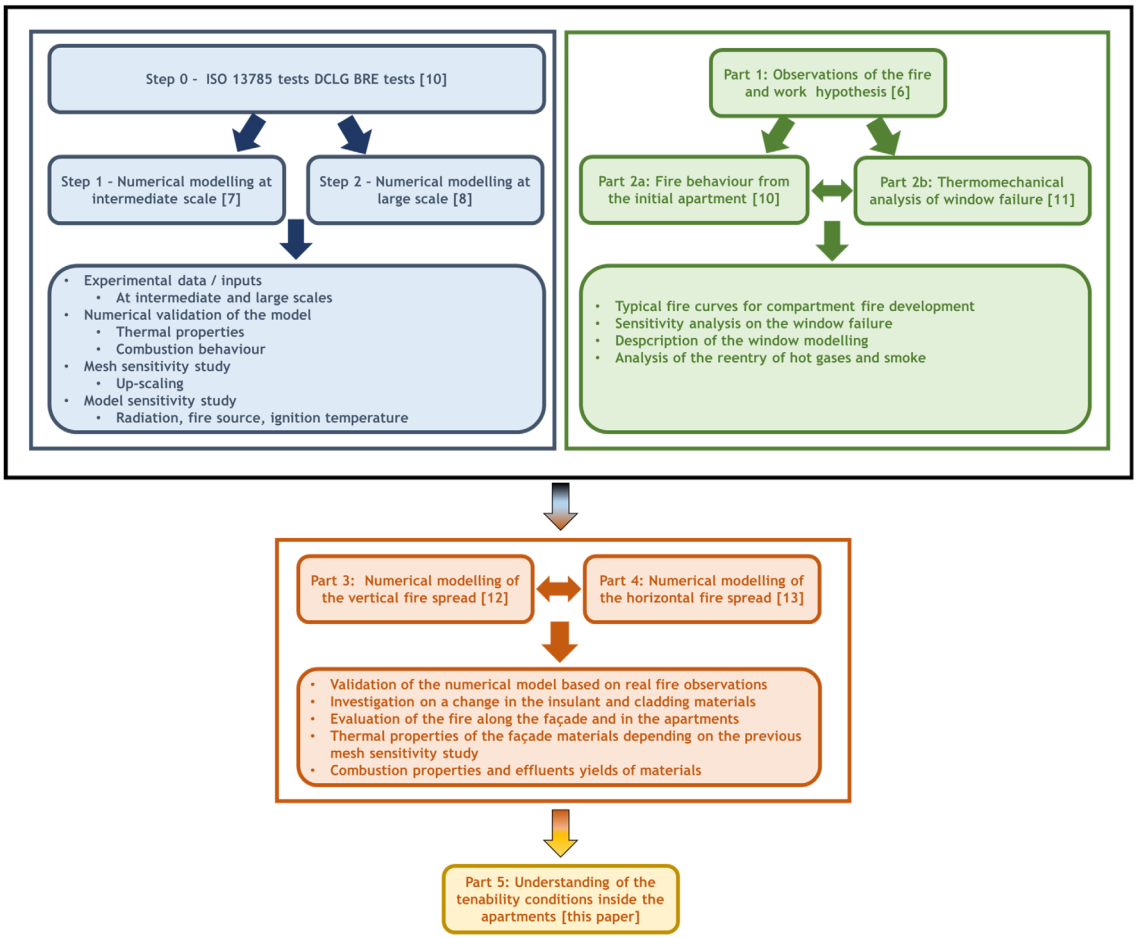

FIGURE 2 Synthesis of the whole approach from the very first step of this research to the actual paper-highly interdependent parts, both experimental and numerical

The Grenfell Tower fire resulted in 71 fatalities. Fire smoke reduces visibility and burns exposed skin, and also burns the mouth and nose if hot air is inhaled. The effects of heat exposure are dose-related and depend on the intensity of heat radiation or smoke temperature and on the duration of exposure. Smoke also contains irritants and asphyxiant gases. At the limit of tenability, irritant species will affect the eyes, nose and throat and cause breathing difficulties. They also affect behaviour to a certain degree, by inducing tears and coughing, and by limiting visibility and movement.[34] The effects of exposure to asphyxiants, including carbon monoxide (CO), hydrogen cyanide (HCN) and carbon dioxide (CO_2), depending on the inhaled dose over a period of time and thus, on the concentrations of these species and on the duration of the exposure. Their effects depend on the variability of human responses to toxicological injuries. Depleted oxygen may also be a parameter driving tenability.[18]

Thus, the contribution of any burning materials in terms of mass loss rate, yields of combustion products, etc., as well as their burning conditions (well or under–ventilated conditions) must be considered to evaluate tenability in terms of toxicity and heat. However, a number of factors complicate the characterization of gases released from a fire. A fire is a dynamic and turbulent process and the concentration of specific compounds in the smoke may change from μl/L to percentage levels during the fire, or from one part of the plume to another. Thus, the composition of smoke gases is often very complex and changes rapidly with temperature and ventilation conditions.[19–33]

For flat configurations such as those at Grenfell, the English Building Regulations, require compartmentation between flats and between flats and common areas. Thus, fire is supposed to be confined in the flat of origin and should not spread into the lobbies or, via the exterior façade, to other flats. The common lobbies should be separated by fire-resistant elements from the main escape stair, at least for 30 min in the event of a fully developed fire. Naturally, this value is highly theoretical and does not consider smoke leakage. However, these measures should prevent smoke from entering the lobbies and stairs, allowing occupants to evacuate in safe conditions without exposure to toxic smoke and heat.

During the Grenfell fire, different combustion ventilation regimes may have occurred. For the external façade system fire, the external cladding is thought to have burned in a well-ventilated regime because the system was directly supplied with oxygen from the exterior. The ventilation regime for the insulant is unknown and probably varied with time, especially being well-ventilated when the external cladding disappeared. For the apartment fires, the main fire source is provided by the furniture. The combustion is assumed to occur first in well-ventilated conditions, because of the ambient oxygen available, followed by a quick transition to an under-ventilated regime. This time scale of oxygen consumption is typical of compartment fires and was evaluated numerically in the previous research dealing with the assessment of representative apartment fires in Grenfell Tower.[10] In particular, the effluent yields for CO and HCN will increase when the oxygen concentration inside the apartment falls below 15%. Other effluents can be considered for toxic evaluation, such as hydrogen chloride (HCl) yield, which is not dependent on ventilation conditions.[32]

3 | NUMERICAL SETUP

In previous work,[6] observational data from the Grenfell Tower disaster were analyzed to provide a synthesis of the vertical and horizontal fire propagation over the whole of the Tower. Vertical and horizontal fire propagation rates were calculated for the different faces of the Tower. The numerical work detailed in references 12,13, investigated the vertical and horizontal fire spread over the façade and into the apartments using a full-scale model of the Grenfell Tower. The fire spread from the façade, into the apartments, through windows, was assessed numerically and validated by comparison with observational data. Thus, the effluent concentrations in each flat of the Tower can be evaluated numerically as a function of time. This paper presents an impact model that considers fire loads from the façade system and from apartment furniture. Tenability conditions are assessed in terms of thermal effects and toxicity and the relative contributions of the façade components and the apartments' contents.

The numerical simulations are performed using FDS version 6.7.0. FDS is a computational code in fluid dynamics that incorporates a combustion model and a large-scale model (LES) for the description of turbulent flows. This tool allows 3D modelling of the computational domain. It considers heat transfer at walls, ventilation conditions for the removal of hot gases, and air intakes. The Navier-Stokes equations are solved in the limit of low Mach number, thermally driven flow with an emphasis on smoke and heat transport from fires. Radiative heat transfer is included in the model through the solution of the radiative transport equation for a grey gas. The default Deardorff model is used for the LES sub-grid modelling. The default sub-models of FDS were used for gas-phase radiation exchanges with 100 (default value) solid angles. The combustion model with primitive and lumped gas species definition to solve a transport equation for each species to be tracked was also investigated. A single-step combustion model was used. It considers a fuel that reacts with oxygen in one mixing-controlled step to form combustion products such as soot and CO. Soot and CO formation yields are inputs of the simulation and selected from the literature and dependent on the studied fire scenario. Without further validation, the multiple steps model for the formation of CO implemented in FDS was thus not used. Fuel burnout in each solid numerical cell is accounted for by the specification of the combustible mass of the object through the bulk density parameter. Thus, when the mass contained in each solid cell is consumed, the solid disappears from the calculation cell by cell. This feature is used to model the destruction of the cladding, as observed experimentally with ACM-PE experiments. The default near-wall model with a wall function for a smooth wall is used. The heat transfer at walls is simulated with a subsequent heat of vaporization to account for the energy loss due to the vaporization of the solid fuel. Every input used in the simulation and not mentioned in the paper are the default ones of FDS, and is deeply

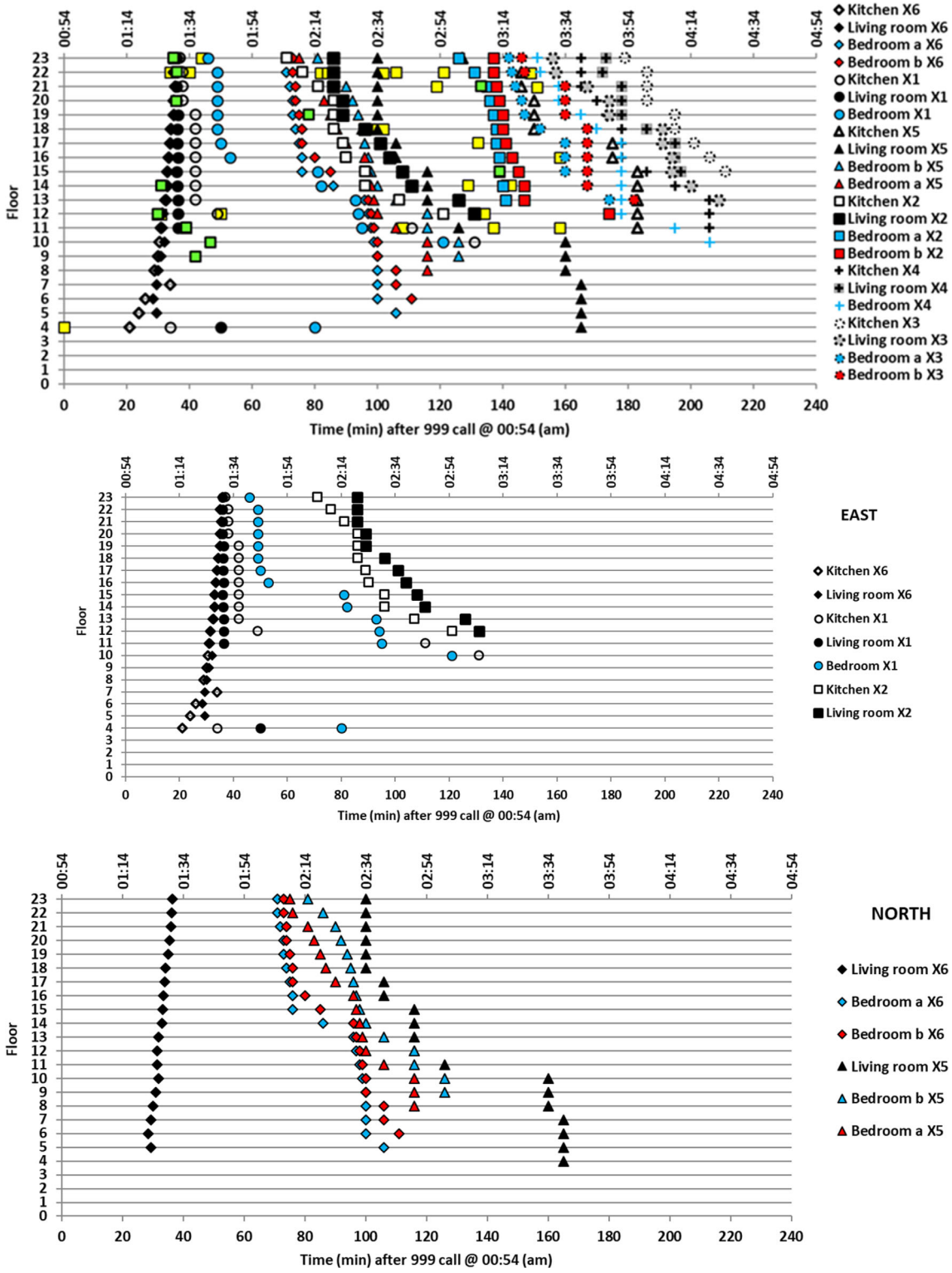

FIGURE 3 Evolution of numerically evaluated window failure times (different symbols depending on the flat position ["X1" to "X6"] and room involved)[13]—Recorded observations of fire (yellow square) or smoke (green square) at a given floor[4]—Numerical simulation for the vertical and horizontal fire propagation over the four faces of the tower at 04:00 a.m.[13]

discussed and indicated in all the previous research dedicated to the numerical work investigating the vertical and horizontal fire spread over the façade and into the apartments using a full-scale model of the Grenfell Tower.[12,13]

In the three-dimensional CFD model of the Grenfell Tower, the thermal and combustion characteristics of the façade system are those validated in references 12,13. Mesh size was uniform and taken as 0.25 × 0.25 × 0.25 m. The heat release rates from the combustion of

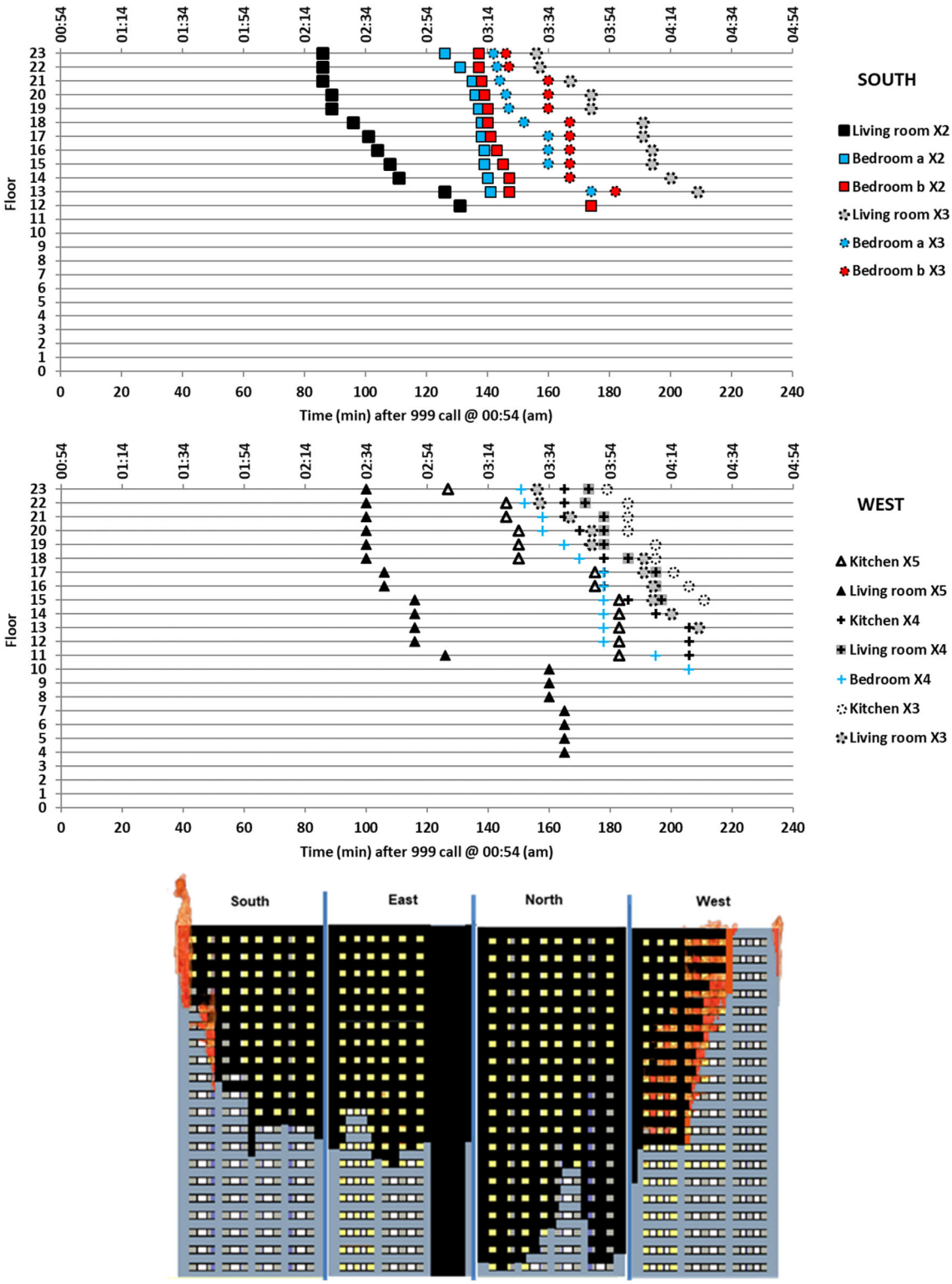

FIGURE 3 (Continued)

apartment furniture, detailed in reference 10, are used for each floor of the Tower. The failure criteria for windows, as assessed in reference 11 are implemented for each apartment opening. In the global model of the Tower, it is assumed that there is no fire propagation path between floors, for example, via ducts, HVAC systems, or holes in ceilings or walls. The fire propagation from one apartment to another (horizontally or vertically) occurs only via propagation over the façade, followed by window failure. In reference 13, a numerical model of fire spread over the four faces of the Tower was validated by comparison with video and photographic records. The fire conditions over time, in terms of burning

condition, window failure, heat release rate and effluent concentrations, are thus known at every location in the façade and inside the apartments (see Figure 2 in reference 13).

The evolution of window failure times, depending on the room involved, is evaluated numerically in reference 13 for the whole Tower. It is compared with records of the presence of fire or smoke at a given floor[4] and allows the understanding of the fire propagation over the Tower. An overview of the window status is illustrated in Figure 3. The failure times for windows on the East face (the face considered in this study) and the other faces of the Tower are shown separately. Thus, for each floor of the Tower, the mass flow rates in and out of a given kitchen, living room and bedroom window, were evaluated numerically.

The local concentrations of every species from combustion can then be calculated in the center of each room (kitchen, living room and bedroom) and for each apartment. The evaluation of flow through windows allows the separate quantification, for a given apartment, of the concentrations of toxic species derived from the façade materials and from the apartment's contents.

During the Grenfell disaster, the refurbished windows were not designed to present any performance against thermal action. In association with the combustible cladding mounted on the façade, it may have facilitated the spread of fire between the interior and exterior of the building. Furthermore, the fallout and deformation of windows and surrounding elements seem to be one of the main elements that has led to the fire spread to the cladding at an early stage of the façade fire spread. Later, when the fire was fully developed, the heat fluxes imparted to the windows were high enough to break the window panes whatever the surrounding materials were (Chapter 24 of reference 2). As concluded by Professor Bisby in reference 2, the most likely route of flame spread, from the initial apartment and then upper ones, had been through the side of the window and into the column cavity following the deforming of the unplasticized polyvinyl chloride (PVC) window surrounds after that the frame was partially failed. However, window failure was probably not the only way of flame exit and re-entry, and the window failure mode is probably not unique during the Grenfell disaster as summarized in Table 1. The scenario leading to one of the earliest massive inflow of fire effluents appears to be the deformation of the window frame and is thus considered in the present work, although that especially when comparing smoke resulting from furniture and from facade materials, the gaps that may exist locally around the window has an influence before the window glass breaks.

4 | IMPLEMENTATION OF THE IMPACT MODELS

4.1 | Fire threat models used

All models used and assumptions are valid for tenability and may differ from those used for lethality. Tenability assessment studies in fire safety engineering are based on an evaluation of the thermal effects and the effects of smoke toxicity. Tenability is defined as the ability of humans to perform cognitive and motor-skill functions at an acceptable level when exposed to a fire environment. It means that occupants in a fire situation should be able to escape by their own devices or to remain safe in specific locations, with acceptable physical and mental capabilities. The limit of tenability is characterized as incapacitation. ISO 13571[34] has been developed as a toolbox to perform tenability analysis. The standard proposes several models to determine the time to compromised tenability for thermal effects and toxicity, among other factors. In such analyses, the time to compromised tenability is the earliest time that is reached for an occupant. Tenability models are often questionable by nature, and this is why two different models have been used in this work: the original one from ISO 13571 and the evolution of it proposed by Pauluhn in 2018.[36,37] The models are used in this study to identify contributors to tenability more than to evaluate absolute tenability conditions in the apartments.

In the present paper, the objective is to use existing models and to compare their results to identify the degree of independence of the conclusion from very different models.

4.1.1 | Thermal models

Thermal effects may be due to the temperature of the air (convective effect) or to the received radiation (radiative effect). Two models are tested in the present publication.

TABLE 1 Synthesis of the main failure modes of the window and resulting consequences during the fire development from reference 11

Failure mode	Main consequences	Resulting inlet	Fire development
Thermal shock on one side of a glass pane	Local glass breakage—first pane in case of double glazing	Reduced	EARLY
Mechanical losses of mounting and fixing such PVC pre-frames	Pathway surrounding the window	Local at surround	
Mechanical stress due to deformation of the frame	Failure of the whole glass pane	Massive	
Thermal gradient at the shaded corners of the glass pane	Local glass breakage—first pane in case of double glazing	Local then massive	LATE
Failure of aluminum supporting rails	Failure of the whole window	Massive	Protected by PIR insulant

Thermal model #1

This model is the original one from ISO 13571.[34] The convective and radiative effects are cumulative and dose-related. The corresponding evaluation criterion that combines these two effects is fractional effective dose due to thermal effects (FED_{therm}). The model has been developed in accordance with the work of Purser[38] and Wieczoreck et al..[39] It is presented in Equation (1), using the hypothesis of lightly clothed people. In this equation, time is expressed in minutes. The incident heat flux q is expressed in kW/m^2 and the temperature T in°C. The uncertainty in this equation is estimated as ±25% in accordance with ISO 13571:2012.

$t_{Irad} = 4.2 \times q^{-1.9}$ if $q > 2.5$ kW/m^2 and $\frac{1}{t_{Irad}} = 0$ if $q < 2.5$ kW/m^2.

$$t_{Iconv} = \left(5 \times 10^7\right) T^{-3.4}$$

$$FED_{therm} = \sum \left(\frac{1}{t_{Irad}} + \frac{1}{t_{Iconv}}\right) \Delta t \tag{1}$$

Thermal model #2

This model is an evolution of the previous one.[36] It separates radiative and convective effects. The model for radiative effects proposes two levels of tenability, related to two levels of burns. This is valid over the range 1.7 to 20 kW/m^2. For predicting time to pain, the model is detailed in Equation (2). Equation (3) presents the model for predicting time to second degree burns. $\dot{q}''$ is the radiant heat flux, expressed in kW/m^2. q^* is a dimensional-resolving constant (value = 1 kW/m^2). In the analysis later in this paper, only the first tenability level (pain) is considered. Radiation effects are cumulative and dose-related as described in Equation (4). The convective stress is mainly expected to cause hyperthermia. Hyperthermia replaces the convective heat threat used in thermal model 1. Hyperthermia may occur rapidly if the heat evacuation capacity of the body is overwhelmed. This is highly dependent on ambient temperature as well as air humidity. Reference 36 does not recommend any value, but a temperature over 60°C for a few minutes in humid air, or 40°C for several hours, is considered sufficient.

$$t_{Irad} = 250 \times \left(\frac{q\prime\prime}{q^*}\right)^{-1,9} \tag{2}$$

$$t_{Irad} = 416 \times \left(\frac{q\prime\prime}{q^*}\right)^{-1,56} \tag{3}$$

$$X_{Irad} = \sum \frac{1}{t_{Irad}} \Delta t \tag{4}$$

4.1.2 | Toxic gas models

The concept of FED and fractional effective concentration (FEC) relate to the manifestation of physiological and behavioral effects in exposed subjects. Two models are used: the existing ISO 13571 model, adapted to fire safety engineering, and another model more adapted to a regulatory pass/fail approach.

Toxic gas model #1

This model is the original one from ISO 13571 in its 2012 revision.[34] It supposes that the asphyxiant gases have a cumulative effect, and the irritant gases have an instantaneous effect at the tenability level. Asphyxiating (or narcotic) effects are cumulative and related to the absorbed dose. They depend on both the concentration of the asphyxiant gas and exposure time. Carbon monoxide (CO) and hydrogen cyanide (HCN) are the only asphyxiant gases considered by ISO 13571. Their effect may be increased by the presence of carbon dioxide (CO_2). The corresponding evaluation criterion is FED due to toxicity (FED_{tox}). Purser[38] and Kaplan et al[40] developed the calculation formula as detailed in Equation (5). In this equation, CO and HCN concentrations are expressed in μL/L and CO_2 concentration as a volume percentage. The time is expressed in minutes. The uncertainty for FED_{tox} is estimated as ±35% in accordance with ISO 13571:2012. Irritating effects are immediate and related to the concentration of irritating gases. The corresponding evaluation criterion is *FEC*. It means that the irritancy of smoke is concentration-related at the tenability level. This hypothesis is not valid at the lethality level. The calculation of *FEC* is described in Equation (6). In this equation, concentrations are expressed in μL/L. F_{irr} is the critical concentration for any irritant to compromise tenability by itself alone. The values of F_{irr} are proposed in ISO 13571 and summarized in Table 2. The uncertainty for *FEC* is estimated as ±50% in accordance with ISO 13571:2012.

$$FED_{tox} = \sum \frac{[CO]}{35\,000} \times v_{CO_2} \Delta t + \sum \frac{([HCN])^{2.36}}{1.2 \times 10^6} \times v_{CO_2} \Delta t \quad \text{with } v_{CO_2} = e^{\frac{[CO_2]}{5}} \tag{5}$$

$$FEC = \sum \frac{[irr.]}{F_{irr}} \tag{6}$$

Toxic gas model #2

This model has been developed recently.[36,37] As in toxic gas model #1, there are toxicity models for asphyxiants and irritants, as their physiological effect is different at the tenability level.

TABLE 2 Critical concentrations used for the FEC model in toxic gas model #1

Factor	Critical concentration (μL/L)
F_{HCl}	1000
F_{HBr}	1000
F_{HF}	500
F_{NO2}	250
F_{SO2}	150
$F_{acrolein}$	30
$F_{formaldehyde}$	250

Nevertheless, they are both based on parametrization using non-lethal threshold values, as recommended nowadays in inhalation toxicology, in alignment with REACH, AEGLs and other state-of-the-art protocols. Some technical aspects are also different. Firstly, CO_2 is considered for its effect, not as an aggravating factor for hyperventilation as in toxic gas model #1. Secondly, irritants are also considered through their dose effect. The general aspect of the model is given in Equation (7), where C_i^n is the average incremental concentration, expressed in μl/L of the class-specific toxic gas I, AF is the assessment factor applied to calculate the incapacitation threshold based on the respective non-lethal threshold concentration, Δt is the chosen time increment, expressed in minutes and k_i is the effect-based toxic load constant. For asphyxiants, the model considers the effect of CO, CO_2 and HCN as in Equation (8). For irritants, the parametrization of the equation is given by Table 3, taken from SLOT-DTLs values.[41]

$$X_{FED} = \sum_{i=1}^{N} \sum \frac{(C_i \times AF_i)^n}{k_i} \Delta t \tag{7}$$

$$FED_{tox} = \sum \frac{([CO \times 3])^{1.77}}{0.498 \times 10^8} \Delta t + \sum \frac{([HCN \times 3])^{1.64}}{0.109 \times 10^6} \Delta t + \sum \frac{3}{e^{11.4 - 1.14 \times \%CO_2}} \Delta t \tag{8}$$

One of the major parameters governing the proposed model is the assessment factor (AF) used by the expert. An AF of 3 has been used for HCN and CO, and an AF of 10 for all irritants, including interspecies difference, intraspecies effects, and the different uncertainties sources. More details on AF are available in references 43–48.

4.1.3 | Significance of FED and FEC values

FED and/or FEC for both model #1 have been established by a median analysis of effects on the population. As a consequence, assessment of any exposed population supposes that the sensitivity across the population is taken into account, even roughly. Without further knowledge, assessment of the population supposes a lognormal repartition of the effects through the population. In other words, the significance of FED and/or FEC = 1 is that the effect would occur for 50% of the normal population. The significance of FED and/or FEC values in terms of coverage of the population is given in Table 4. Such an approach is very useful for probabilistic studies but does not allow certainty of coverage of the population, and as a consequence is difficult for regulators to accept.

FED for both model #2 is based on non-lethal endpoints. Contrary to the previous FED model for asphyxiants, parametrization indicates that the incapacitating effect of CO and HCN occur at one-third of the lethality endpoint. The effect of CO_2 is considered in its own right. For irritants, the model is dose-based so only cumulative. Regarding the parametrization of the AF factor, it estimates that the incapacitation effect occurs at 1/10 of the lethality endpoint. The factor AF is selected by the user, but toxicological knowledge is required to make this selection properly. The coverage factor of such a model is very different from the previous one. Probabilistic assessment is lost for such a model based on pass/fail tenability criteria. Below FED = 1, no effect is supposed to occur in a normal population. Over FED = 1, effects start to occur. This kind of approach is ideal for a pass/fail assessment. It is used in inhalation toxicology and for many regulatory purposes, such as the REACH regulation in the EU, as it covers fully the general population.

Regarding the hypotheses presented, FED = 1 in model #2 is supposed to have approximately the same coverage factor as FED = 0.1 in model #1.

4.1.4 | Oxygen depletion model

Interpretation of effects due to dioxygen depletion is also included in the analysis. A threshold of 16% of dioxygen is considered as a concentration sufficient to compromise tenability in a few minutes.[42,43]

TABLE 3 Parametrization for irritants in toxic gas model #2

Component	*n*	k [(μl/L)^n × min]	AF
Acrolein	1	420	10
Bromine	2	2.5×10^5	10
Chlorine	2	1.08×10^5	10
Fluorine	2	3.8×10^5	10
Formaldehyde	1	5700	10
Hydrogen bromide	1	1.22×10^4	10
Hydrogen chloride	1	2.37×10^4	10
Hydrogen fluoride	1	1.2×10^4	10
Nitric oxide	1	2.09×10^4	10
Nitric dioxide	2	9.06×10^4	10
Sulphur dioxide	2	4.66×10^6	10

TABLE 4 Significance of FED and/or FEC criteria for thermal and toxic gas model #1

	Significance:	
FED and/or FEC value	% of the population considered as occurring the effect	% of the population considered as protected from the effect
0,1	1.1%	98.9%
0,2	5.4%	94.6%
0,3	11.4%	88.6%
0,5	24.4%	75.6%
1,0	50.0%	50.0%
1,5	65.7%	34.3%
2,0	75.6%	24.4%

4.2 | Fuels and effluents scalar data monitored

Each chemical species of interest has been monitored through a transport equation solved by the fuel of origin. Species generated are representative of the materials involved as well as ventilation conditions. The technical choice has been made to monitor effluents from the various products present in the façade, at windows reveals and inside the apartments, as presented in Table 5. All calculations also consider soot as essential in radiative transfer, and in thermal impact models.

The furniture contribution was estimated in a previous study[10] and considered the combustion of tables, chair, a carpet, sofas, a TV set, a wardrobe, a mattress, nightstands and electronic devices (a washing machine, a cooker a fridge freezer and a mini-fridge). The main gases that were considered are wood, polyethylene, polycarbonate and poly-urethanes. The main gases are hence CO_2, CO and HCN.

Each quantity is evaluated in the middle of a room, at a height of 1.5 m, corresponding to typical mean nose and face height.

4.3 | Gas yields used for toxic threat assessment

During the Grenfell fire, several different combustion ventilation regimes may have occurred. For the external façade system fire, the external ACM-PE cladding is thought to have burned in a well-ventilated regime because the system was directly supplied with oxygen from the exterior and disappeared quickly. This is also thought to be the case for window infill panels. This is also compatible with the observations addressed during the intermediate scale tests.[7] For the poly-isocyanurate (PIR) façade insulant and window's reveal insulant, ventilation regimes vary with time and fire spread.

The HCl yield of the PVC window reveals lining is not dependent on vitiation conditions and remains constant whatever the conditions are.[50] The yields used for this product in the study are 0.27 g/g for HCl, 0.063 g/g for CO and 0.176 g/g for soot.[10,12,49] The heat of combustion and heat release rate per unit area were provided in reference 49.

All the combustion properties for the cladding material (ACM-PE), the window reveal insulant (PIR W) and the infill panels (XPS), in terms of CO, HCl and soot yields, the heat of combustion and heat release rate per unit area, are those used in previous studies of the Grenfell tower fire and detailed in associated references [7, 8, 10, 12, 13].

A summary of the yields for the gas species considered is given in Table 6.

Initially, for the façade insulant, under-ventilated conditions would probably have quickly developed in the cavity. Then, due to the quick combustion of the external cladding, the conditions probably changed (Figure 4). Yields corresponding to under-ventilated conditions were chosen initially for the facade insulant, assuming the air available inside the cavity is negligible. Then, when the ACM-PE disappears, the conditions are assumed to be well-ventilated. The duration of combustion of the ACM-PE cassettes is limited and has been assumed to be 5 min at each location on the basis of ISO 13785-1 test data.[7,9] During these tests, ACM-PE panels with dimensions close to 530 $\times$ 780 mm were observed burning for a maximum of 3 min. CFD modelling[7] reproduced these observations well, and this modelling showed that the PIR insulant behind the cladding was involved in the fire for 2 to 3 min. In less than 8 min, all the ACM-PE panels had disappeared. The contribution of the insulant was found to be 5% of the cladding heat release rate measured during the test. Similar observations were made at larger scales in reference 8, where the contribution of the insulant represented a maximum of 7% of the numerically evaluated system HRR during the test. The ACM-PE panels contributed to the fire until their complete consumption in 4 min. Thus, the 5 min assumed for the involvement of the ACM-PE in this study is quite reasonable

TABLE 5 Considered products and associated gas species for emission

Product	Location	Transport equation abbreviation	Species scaled
PIR facade insulant	Façade	PIR	CO_2, CO, HCN
ACM-PE cladding	Façade	PE	CO_2, CO
Window infill panels	Façade	XPS	CO_2, CO
PVC window reveal lining (rigid)	Window frames	PVC	CO_2, CO, HCl
PIR window reveal insulant	Window frames	PIR W	CO_2, CO, HCN
Furniture	Inside apartments	Furniture	CO_2, CO, HCN

TABLE 6 Yields of the gas species considered, except for apartment furniture and PIR

	Abbreviation	[CO] (g/g_{fuel})	[HCN] (g/g_{fuel})	[HCl] (g/g_{fuel})	[soot] (g/g_{fuel})
ACM-PE (cladding)	PE	0.024	–	–	0.056
Window infill panels	XPS	0.060	–	–	0.200
PVC window reveal lining (rigid)	PVC	0.063	–	0.270	0.176
PIR window reveal insulant	PIR W	0.031	0.010	–	0.130

giving regard to the dimensions of the cassettes and the severity of the façade fire (Figure 4).

Figure 5B collates data, from the simulations of the whole East face of the Tower,[12] on the difference in times to ignition of the different surfaces within the façade system as a function of their location. The simulations performed in references 12,13 showed that when the ACM-PE cladding panels ignite (internal face), the PIR insulant ignites between 0 and 0.5 min after except for the first floor (PE− to PIR+ in Figure 5B). The delays correspond to the time difference between the ignition of the exposed face of the ACM-PE cladding (PE+), the unexposed face of the cladding (PE−), and the exposed face of the insulant (PIR+) as shown in Figure 5A). Below Floor 6, PE+ ignites before PE− and before PIR+. Therefore, the PIR insulant will be exposed to fire quickly after the ACM-PE panels have been involved and have disappeared. From these simulations, the contribution of the insulant represented a maximum of 5.5% of the numerically evaluated system HRR during the first vertical phase of the fire spread over the East face of the Tower.

A burning duration in the range of 5 min was observed in the simulations. During this period, the oxygen concentration in the cavity and near the insulant indicated under-ventilated conditions (Figures 6 and 7), until the ACM_PE disappears. After the ACM-PE panels disappeared, the PIR insulant continued to burn in well-ventilated conditions, under the influence of the external flames from the burning contents of the apartment.

For the apartment fires, the furniture provides the main source of combustion gasses. The combustion is assumed to occur first in well-ventilated conditions, because of the ambient oxygen available, followed by a quick transition to an under-ventilated regime. The effluent yields for CO and HCN will increase when the oxygen concentration inside the apartment falls below 15%.

An extensive bibliographic study was then conducted to investigate the CO and HCN yields appropriate for apartment furniture and the façade insulant. The apartment furniture is assumed to be an average of wooden and flexible PU foam items. The yields for several test methods and ventilation conditions (in the case of apartment furniture)[19–33] were evaluated. This gave a range of values. The minimum (MIN), average (AVE) and maximum (MAX) of that range of values for CO and HCN yield are indicated in Tables 7 and 8. Thus, different yield assumptions can be evaluated with the impact models. The average value is calculated from the full set of yields available from the extensive bibliographic study.

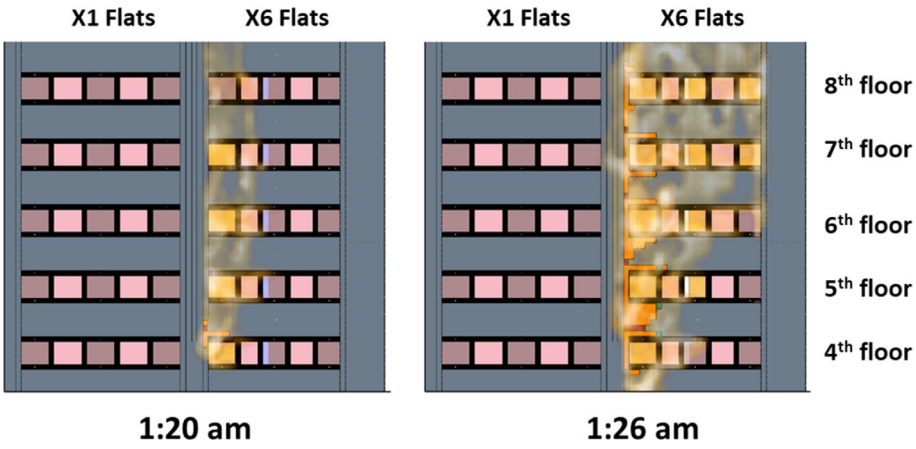

FIGURE 4 Visualization of the simulation of the fire between the 4th and the 8th floors on the East face of the Tower[13] soon after the fire spread to the facade—parts of the external cladding are missing, insulant (orange surfaces) is exposed to the flames

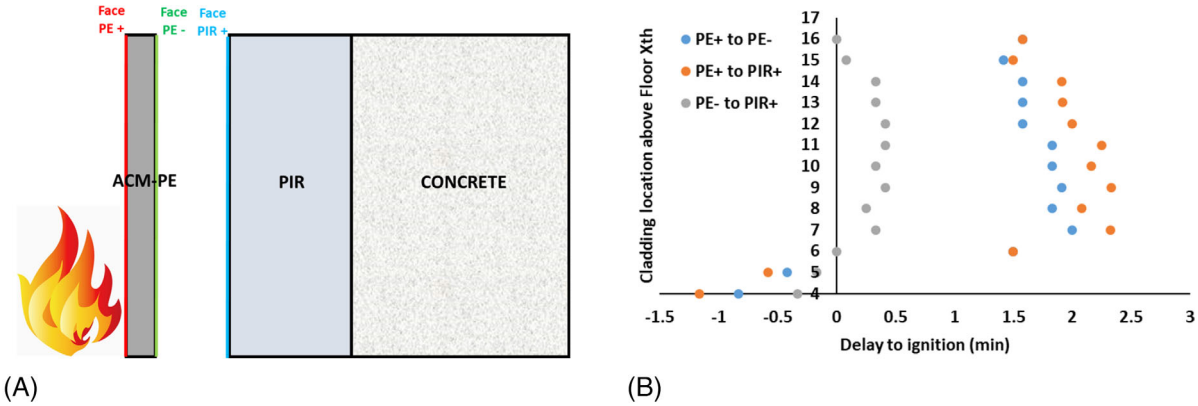

FIGURE 5 Data, from the simulations of the whole East face of the Tower,[12] on the delay in the ignition of the different surfaces within the façade system as a function of their location between the 4th and the 16th floors

4.4 | Combustion gas yield assumptions investigated

Three different combustion gas yield assumptions have been investigated for each of the apartment furniture and the PIR façade insulant.

A summary of the nine combined combustion gas yield scenarios is indicated in Table 9. The toxicity FEDs have been evaluated with the two toxicity models #1 and #2. The authors estimate scenario 1 as the most severe and scenario 6 as the central one, so the detailed results for these two scenarios are presented in the following sections, even though the nine scenarios have been calculated.

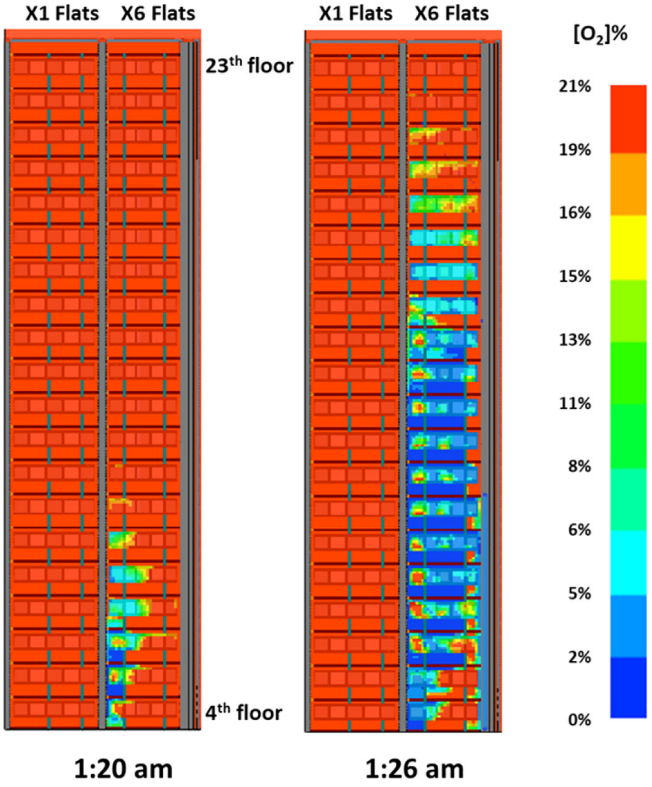

FIGURE 6 Calculated oxygen volume percent in the cavity between the ACM-PE panels and the PIR insulant between the 4th and 23th floors from the simulations of the whole East face of the Tower[13]

5 | QUANTIFICATION OF FIRE EFFLUENTS AND APPLICATION OF THE IMPACT MODEL

5.1 | Selected flats for the application of the impact model

Three apartments in the "X6" position, were analyzed during the vertical propagation of the fire over the east face of the Tower, between 01:05 and 01:29 a.m. They are identified in Figures 8–10. Flat 26 is located on the 5th floor, just above the apartment of origin of the fire. Flat 96 is located on the 12th floor, at mid-height of the Tower. Flat 196, on the 22nd floor, is located near the top of the Tower. Observations provided in Prof J. Torero's expert report[4] give the times of window failure for flats 26, 96 and 196 as 01:18 a.m., 01:25 a.m. and 01:28 a.m., respectively. These times are consistent with the numerical predictions in reference 12.

For each floor of the Tower, the mass flow rates in and out of a given kitchen, living room and bedroom window, were evaluated numerically. The local concentrations of every species detailed in Table 5 were calculated in the center of each room (kitchen, living room and bedroom), for each apartment, at a height of 1.5 m (corresponding to the position of the human nose, mouth and eyes). The evaluation of flow through windows allows the separate quantification, for a given apartment, of the concentrations of toxic species derived from the façade materials and from the apartment's contents.

5.2 | Influence of mesh refinement

The simulation of the whole fire requires a coarse mesh to allow modelling to be completed on an acceptable timescale. So, before conducting

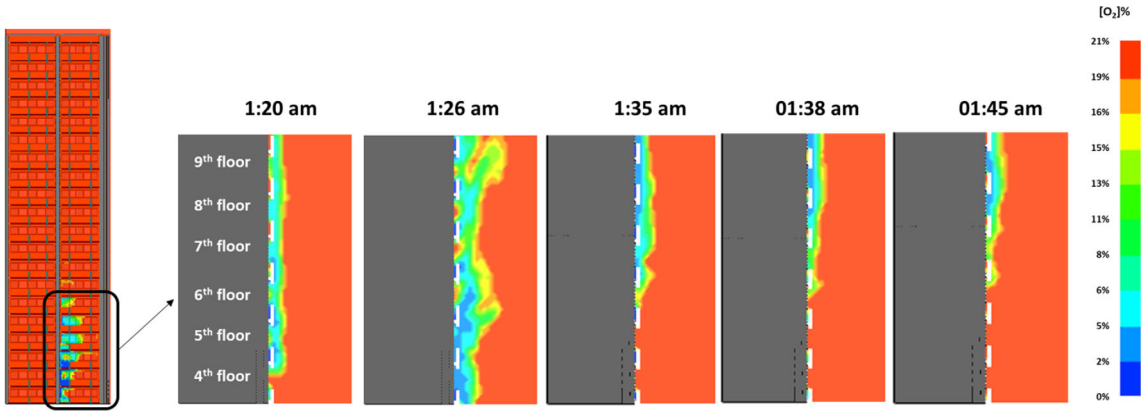

FIGURE 7 Details of the calculated oxygen volume percent in the axis of the kitchens of "X6" flats between the 4th and 9th floors from the simulations of the whole East face of the Tower[13]—the cavity between the ACM-PE panels and the PIR insulant is visible

TABLE 7 Summary of the literature review for the CO and HCN yields [g/g_{fuel}] depending on ventilation conditions for apartment furniture[19–33]

		Well-ventilated (WV)		Under-ventilated (UV)	
		[CO]	[HCN]	[CO]	[HCN]
Apartment furniture	MAX	0.060	0.006	0.290	0.013
	AVE	0.037	0.003	0.160	0.007
	MIN	0.015	0.001	0.029	0.001

TABLE 8 Summary of the CO and HCN yields [g/g_{fuel}] depending on ventilation conditions for the PIR façade insulant from various test standards from reference 19

		Well-ventilated (WV)		Under-ventilated (UV)	
		[CO]	[HCN]	[CO]	[HCN]
PIR façade insulant	MAX	0.070	0.0050	0.350	0.025
	AVE	0.060	0.0045	0.210	0.015
	MIN	0.050	0.0040	0.070	0.005

TABLE 9 Summary of the investigated scenarios and yields considered for all products studied—Influence of the ventilation (WV for well-ventilated, UV for under-ventilated) depending on the window breakage time (t_i) for criteria of 15% of O_2 concentration in a room

SCENARIO	Yields for the apartment furniture Values taken from Table 6 (furniture)	Yields for the PIR façade insulant values taken from Table 7 (PIR)	Yields for the internal parts of the façade (PIR W—PVC)	Yields for the external parts of the façade (PE—XPS)
1	MAX $^{>15\%O_2\rightarrow WV}_{\leq 15\%O_2\rightarrow UV}$	MAX $^{t_i-5\,min\rightarrow UV}_{t_i+5\,min\rightarrow WV}$	Values taken from Table 5 for these products	Values taken from Table 5 for these products
2	AVE $^{>15\%O_2\rightarrow WV}_{\leq 15\%O_2\rightarrow UV}$	MAX $^{t_i-5\,min\rightarrow UV}_{t_i+5\,min\rightarrow WV}$		
3	MIN $^{>15\%O_2\rightarrow WV}_{\leq 15\%O_2\rightarrow UV}$	MAX $^{t_i-5\,min\rightarrow UV}_{t_i+5\,min\rightarrow WV}$		
4	MAX $^{>15\%O_2\rightarrow WV}_{\leq 15\%O_2\rightarrow UV}$	AVE $^{t_i-5\,min\rightarrow UV}_{t_i+5\,min\rightarrow WV}$		
5	MAX $^{>15\%O_2\rightarrow WV}_{\leq 15\%O_2\rightarrow UV}$	MIN $^{t_i-5\,min\rightarrow UV}_{t_i+5\,min\rightarrow WV}$		
6	AVE $^{>15\%O_2\rightarrow WV}_{\leq 15\%O_2\rightarrow UV}$	AVE $^{t_i-5\,min\rightarrow UV}_{t_i+5\,min\rightarrow WV}$		
7	MIN $^{>15\%O_2\rightarrow WV}_{\leq 15\%O_2\rightarrow UV}$	MIN $^{t_i-5\,min\rightarrow UV}_{t_i+5\,min\rightarrow WV}$		
8	AVE $^{>15\%O_2\rightarrow WV}_{\leq 15\%O_2\rightarrow UV}$	MIN $^{t_i-5\,min\rightarrow UV}_{t_i+5\,min\rightarrow WV}$		
9	MIN $^{>15\%O_2\rightarrow WV}_{\leq 15\%O_2\rightarrow UV}$	AVE $^{t_i-5\,min\rightarrow UV}_{t_i+5\,min\rightarrow WV}$		

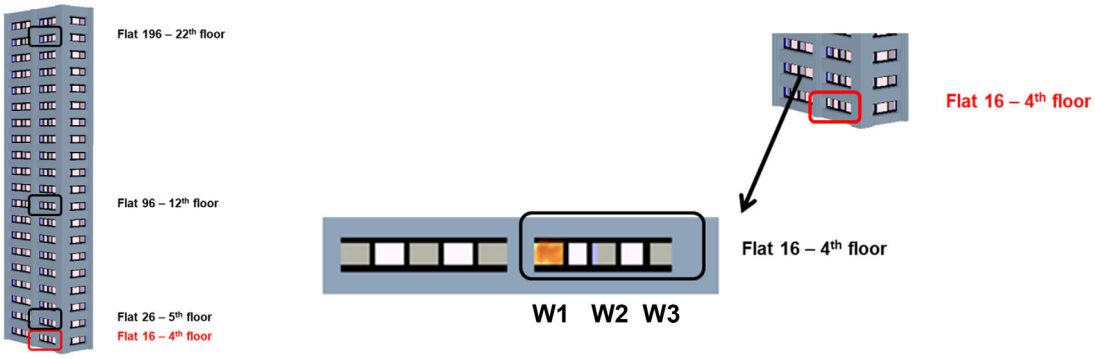

FIGURE 8 Identification of the analysed apartments and windows (W) on the east and north faces of the Tower

the analysis of species concentrations inside the selected flats using the full-scale Grenfell Tower model, the coarse mesh was validated for gas interaction with the apartments by upscaling, in the same way as for heat and flame spread in previous research steps.[10,12,13]

A comparison of inward and outward flows was conducted for flat 26 using the fine mesh CFD model detailed in references 10,12 (see Figure 11). This also allowed validation of the vitiation of this apartment, especially through oxygen concentration. A comparison

between the fine and coarse mesh models for the flow through the kitchen window of flat 26 shows a similar range of values both for incoming and outgoing mass rates. The coarse mesh model seems to over predict the incoming flow from the exterior to the interior of the apartment. The effluent concentrations from the façade fire will therefore be overestimated in the following analysis. The time to oxygen concentration below 15% is also a little quicker, so a slight overestimation of the toxicity from the furnishing is expected.

Using the coarse mesh model, the incoming and outgoing flow through the window show some variations in their amplitude not observed using the fine grid local model. This is due to the difference in the dimension of the numerical cells (0.25 and 0.05 m in this case) on which the flow is calculated.

The coarse mesh model seems to over predict the incoming flow from the exterior to the interior of the apartment, and thus that the effluent concentrations from the façade fire will therefore be overestimated in the analysis. The toxicity analysis presented in this paper in Section 5.3 was performed for the Fat 26 using the model ran with the fine and the coarse meshes. Few differences were observed so that confidence in the analysis for the higher flats is expected (Table 10).

5.3 | Application of the impact model for Flat 26 and Flat 196

Flat 26 is located on the 5th floor, east face, just above the initial fire compartment (Flat 16). Numerical predictions and observations[4] agree on the time of total window failure, leading to apartment ignition, being 01:18 a.m. for the kitchen (window n°3—see Figure 8), and 01:22 a.m. for the living room (window n°2 - see Figure 8). For the kitchen, the global flow through window n°3 travels mainly from the apartment to the exterior, especially when the fire ignites in the

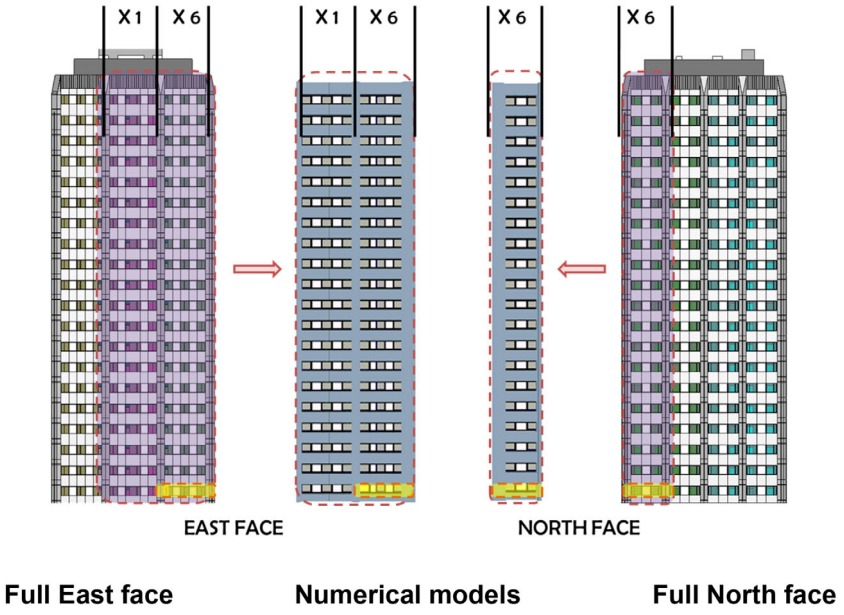

FIGURE 9 View of the numerical model of the Grenfell Tower−−part of the east face with "X6" and "X1" flats—part of the north face with the living room of flats "X6"—Flat 16 is highlighted in yellow

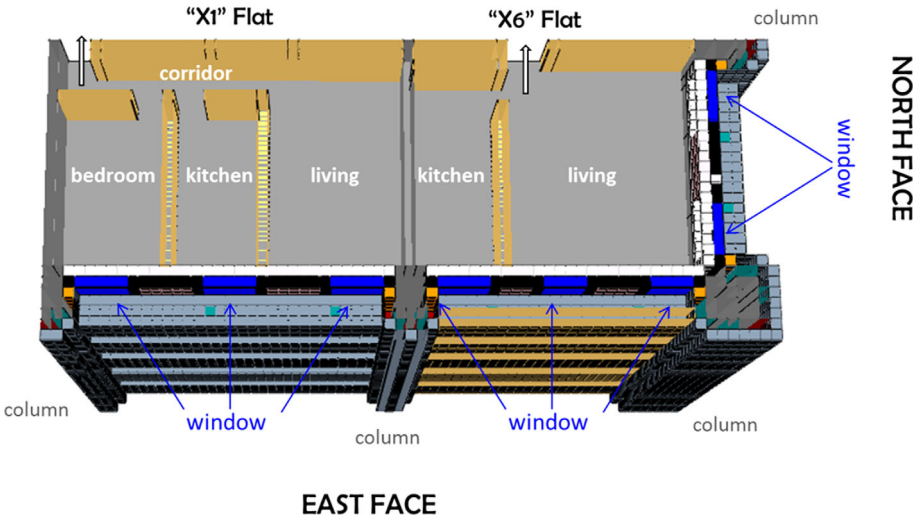

FIGURE 10 View of the numerical model inside the Grenfell Tower—part of the east face with "X6" and "X1" flats—part of the north face with the living room of flats "X6"

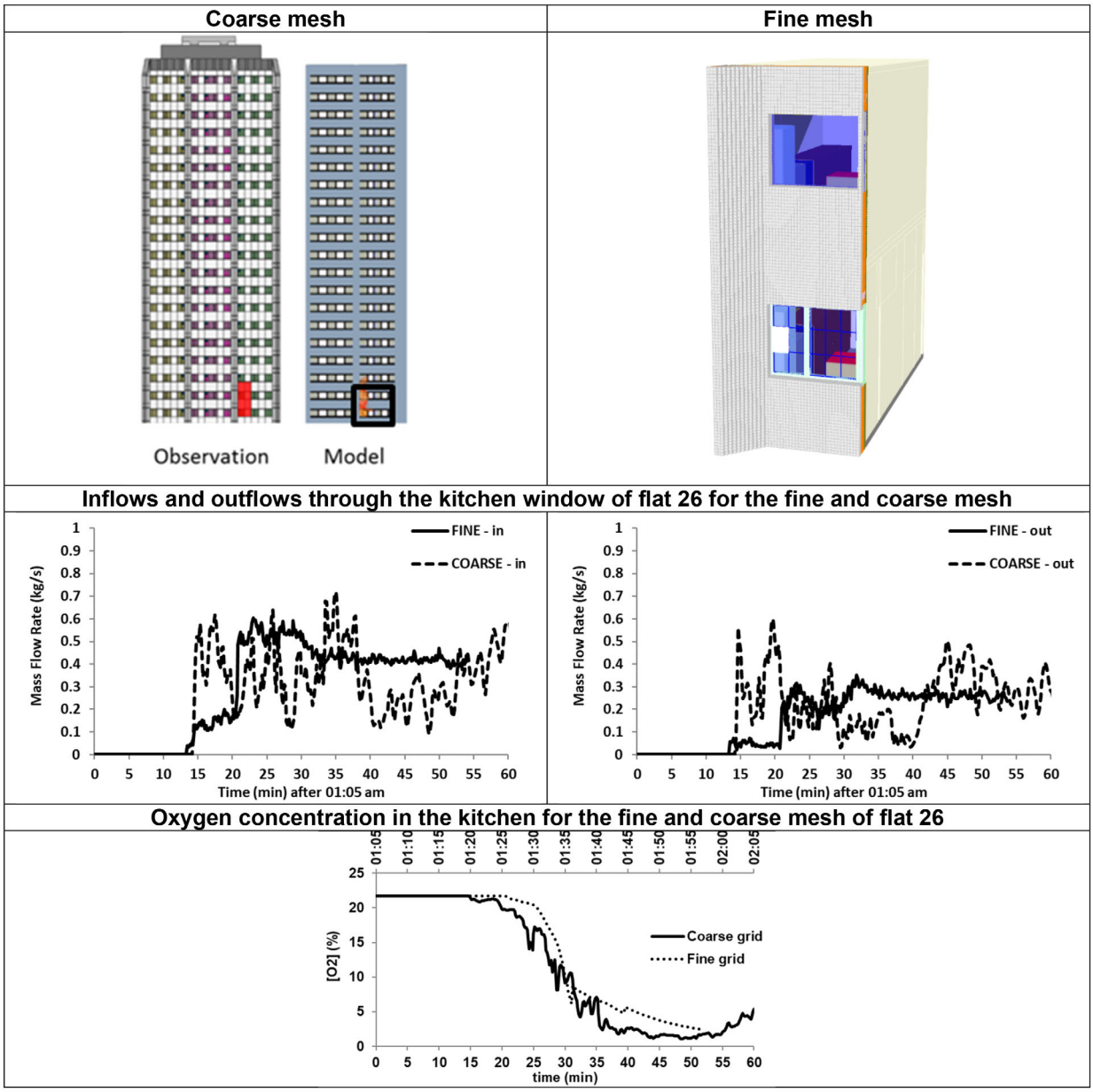

FIGURE 11 Comparison between the coarse and fine mesh models of the incoming and outgoing flows, and oxygen concentration, for Flat 26

kitchen. This is due to air entrainment by the vertical façade fire and the fire plume located mainly between the column and the kitchens of the east face. For the living room, the global flow through the window n°2 travels mainly from the exterior to the apartment. This is due to the air entrainment into the kitchen as a consequence of the global flow out of the kitchen window (window n° 3) and the need for pressure equalization. No breakage of window n°1 (see Figure 8) occurs.

Flat 196 is located on the 22nd floor near the top of the Tower. Numerical predictions and observations[4] also agree on the time of total window failure, leading to apartment ignition, being 01:29 a.m.

TABLE 10 Summary of the investigated cases concerning the incoming and outgoing flow rates after window breakage—averaged over 45 min

	Coarse mesh	Fine mesh
Average incoming flow rate (kg/s)	0.56	0.41
Average out coming flow rate (kg/s)	0.27	0.25
Time to reach 15% in $[O_2]$ concentration	01:32 a.m. (14 min after window failure)	01:34 a.m. (16 min after window failure)

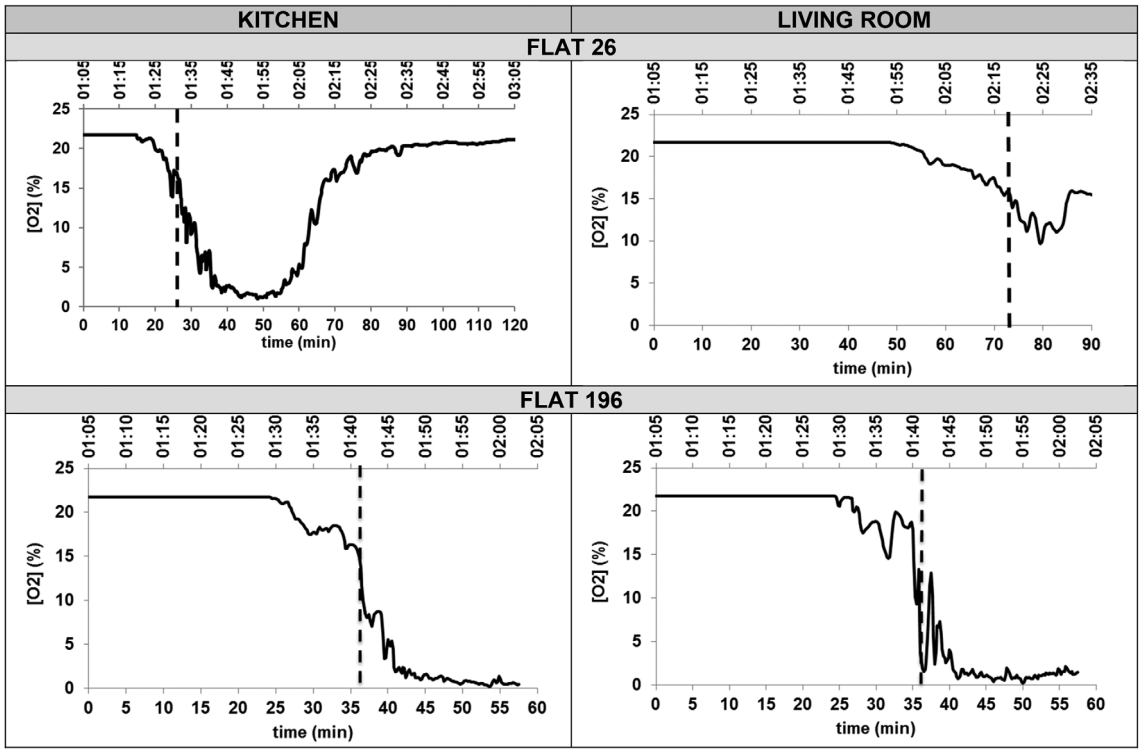

FIGURE 12 Oxygen concentrations evaluated numerically at a height of 1.5 m in the center of the kitchens and living rooms of Flats 26 and 196—Scenario 1

	Flat 26		Flat 196	
Timescale	**Kitchen**	**Living room**	**Kitchen**	**Living room**
Window failure	01:18 a.m.	01:22 a.m.	01:29 a.m.	01:30 a.m.
Under-ventilation	01:32 a.m.	02:16 a.m.	01:42 a.m.	01:42 a.m.
Relative delay	14 min	54 min	13 min	12 min

TABLE 11 Calculated timing of under-ventilated conditions for Flats 26 and 196—Scenario 1

for the kitchen (window n°3), and 01:30 a.m. for the living room (window n°2). For the kitchen, the global flow through window n°3 travels mainly from the apartment to the exterior, especially when the fire ignites in the kitchen. This is due to air entrainment by the vertical façade fire and the fire plume located mainly between the column and the kitchens of the east face. To explain this at a more detailed level, the large flow velocity of the fire is just outside the kitchen window and at the point of window failure the flow travels from the exterior and recirculates into the kitchen. After kitchen fire ignition, the flow travels in both directions but the outward flow dominates. For the living room, the global flow through windows n°2 and n°1 travels mainly from the exterior into the apartment. The large flow velocity behind the window from the fully developed façade fire leads to the flow from the exterior and from the adjacent kitchen and recirculates into the living room. This massive smoke entrainment from the fully developed façade fire explains the differences observed with Flat 26.

Species concentrations in Flat 26 and Flat 196 are evaluated numerically at a height of 1.5 m, and in the center of the kitchen and of the living room for all gas yield scenarios. The example below is for scenario 1 as given in Table 9. The oxygen concentrations are given in Figure 12. Under-ventilation occurs in the kitchen and living room of Flats 26 and 196 at the times indicated in Table 11. For Flat 196, window failure and oxygen depletion inside the living room and kitchen are observed at similar times due to a wider fire plume near the crown of the Tower impinging on both rooms more or less simultaneously. For Flat 26, a time lag is predicted due to the need for the fire to spread horizontally from the original fire plume. Thus, the living rooms of higher X6 flats, such as Flat 196, are involved earlier than those from lower floors.

For the kitchen and the living room of Flat 26, the total value and the detail of species released for each burning material involved show similar conclusions (Figure 13). In the kitchen, the CO is released mainly by the apartment furniture. The HCN is mainly released from furniture and, in the early stages, the PIR window reveals insulant, with a small contribution from the PIR façade insulant. In the living room, the CO is released mainly by the apartment furniture, and to a lesser extent by the PVC window reveal lining. The HCN comes mainly from the apartment furniture with small but insignificant contributions from the PIR insulants.

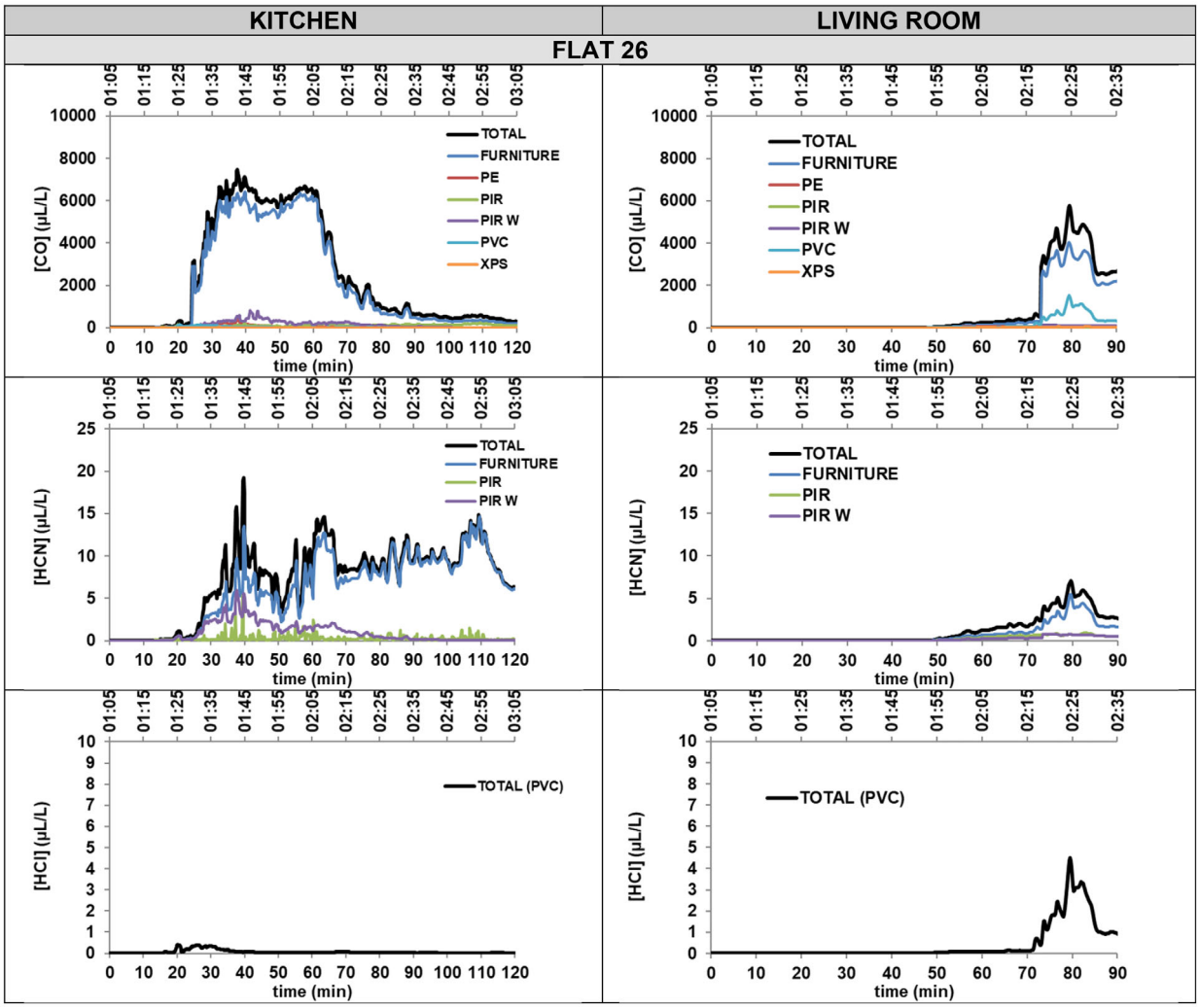

FIGURE 13 Species concentrations and main contributors in the kitchen and living room of Flats 26 and 196—gas yield scenario 1

The results are different for Flat 196 (Figure 13). In the kitchen and the living room, the release of the PVC from the window reveals lining and the PIR window reveals insulant are negligible. In the kitchen and living room, the CO is released mainly by the apartment furniture, after the first income from the façade fire when the window failed. The HCN is mainly released from the apartment furniture and from the PIR façade insulant in similar low concentrations under 20 µl/L.

FEDs and FECs were calculated for the kitchen and living room of Flats 26 and 196 using toxic gas models #1 and #2. By way of example, the toxic gas FED calculation for the kitchen of Flat 26 is shown in Figure 14 for both toxic gas models. Thermal FEDs, according to thermal models #1 and #2, are also indicated.

The times at which tenability became compromised for the first criterion (thermal or toxic) are shown in Table 12. Relative differences between 1 and 10 min are observed between models #1 and #2, with tenability compromised first with model #2 except for the kitchen of Flat 26. The first criterion reached (thermal or toxic) is the same for the living room in Flat 26 and the kitchen in Flat 196. For the kitchen in Flat 26 and the living room in Flat 196 the first criterion reached depends on the model used.

However, for each apartment investigated, for both models (#1 or #2) used, and regardless of which criteria (thermal or toxic) first caused the loss of tenability, the dominant contribution to FEDs and FECs comes from the apartment furniture when involved in the fire.

Because the coarse mesh model seems to over predict the incoming flow from the exterior to the interior of the apartment, and thus that the effluent concentrations from the façade fire as discussed in Section 6.2, the toxicity analysis was performed for the Fat 26 using the model run with the fine and the coarse meshes. Few differences were observed as indicated in Figure 15 so confidence in the analysis for the higher flats is expected.

5.4 | Analysis of contributors to smoke toxicity inside the apartments

A summary of the times to reach under-ventilation and the times at which tenability became compromised for the first criterion (thermal or toxic) is shown in Table 13 for Flats 26, 96 and 196, for the two

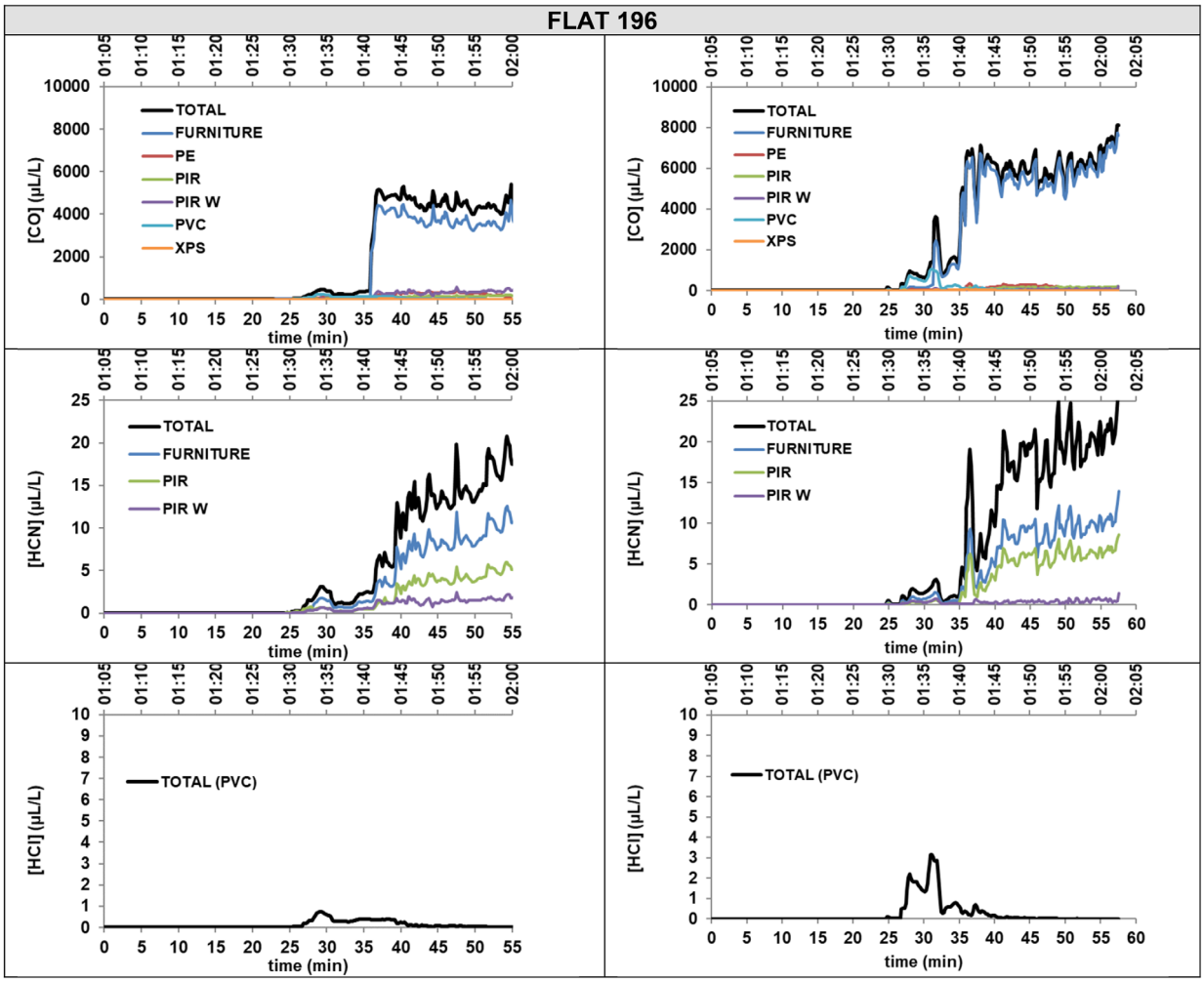

FIGURE 13 (Continued)

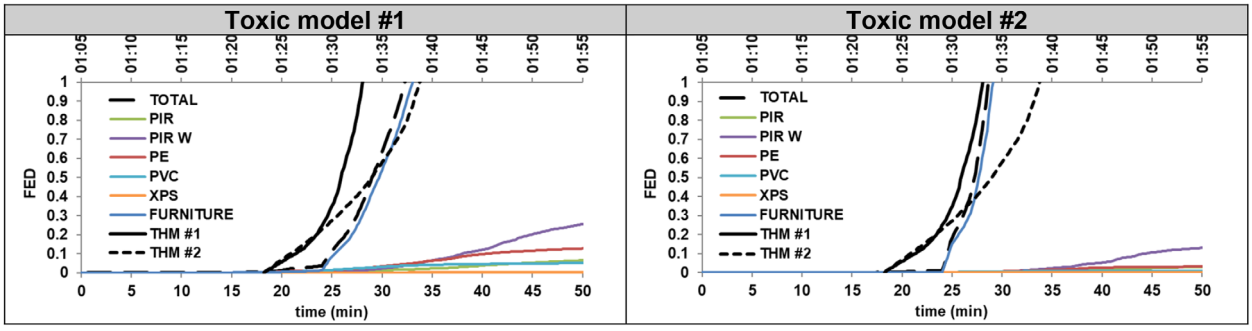

FIGURE 14 Example of FED evaluated numerically at 1.5 m high in the center of the kitchen of flat 26 following 2012 and 2018 revisions of ISO 13571 Standard—Gas yield scenario 1

thermal and toxic gas models and for all gas yield scenarios. Oxygen depletion is reached first, or at a similar time to the thermal FED reaching 1, for the majority of the apartments and scenarios, except for the living room of the lower floors (Flats 26 using model #2 and 96 using model #1). The thermal FED evaluated using the two thermal models reaches 1 before the toxic gas FED for the majority of scenarios and locations inside the apartments, and is due to the apartment furniture's involvement in the fire. For the 54 cases investigated with Model #1, 40 occurrences of thermal criteria reached the first appearance, and thus represent 75% of the investigated scenarios. For model #2 the respective figures are 29 out of 54 cases (54%).

However, smoke propagation from the first impacted apartments to the rest of the structure may increase the impact of the toxicity of

TABLE 12 Time at which tenability became compromised for the first criterion—estimated from conditions in Flats 26 and 196—Gas yield scenario 1

Time at which tenability became compromised for the first criterion (expressed in time)	Flat 26		Flat 196	
	Kitchen	Living room	Kitchen	Living room
Model #1	01:33:00 (thermal criterion)	02:25:00 (thermal criterion)	01:47:00 (toxic criterion)	01:43:00 (thermal criterion)
Model #2	01:34:00 (toxic criterion)	02:15:00 (thermal criterion)	01:43:00 (toxic criterion)	01:41:00 (toxic criterion)

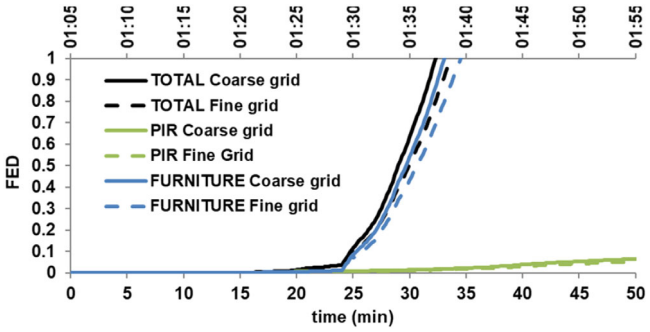

FIGURE 15 Example of FED evaluated numerically at 1.5 m high in the center of the kitchen of flat 26 using coarse and fine meshes—Gas yield scenario 1-2012 revision of ISO 13571 Standard

that smoke and reduce that of thermal conditions as smoke is cooled down and diluted with distance from the apartments. This justifies a deeper analysis of smoke toxicity sources. The main contribution to the toxic criteria evaluated comes from the apartment furniture in every scenario and location as observed in Figure 14.

Average (AVE), minimum (MIN) and maximum (MAX) values for the time at which tenability became compromised by gas toxicity (toxic FED = 1) for the nine gas yield scenarios investigated (Table 9) using the two toxic gas models are given in Table 14 and shown in Figure 16. For every scenario investigated, the maximum FEC or FED associated with irritants is negligible for both toxic models in both the kitchen and living room (Figure 14).

Gas yield scenario 1 is most severe for both the façade insulant and the apartment furniture. The relative influences of the main contributors to the toxic gas FED are shown for 5 and 15 min after window breakage (WB), and at the time for toxic FED = 1 in the kitchen of flats 26, 96 and 196 (Figure 17). Only the toxic gas model #1 is used for this illustration. It appears that the combustion products from the PE (cladding) are present in flat 26 following window breakage and present, but less so, in flats 96 and 196. PVC combustion products are mainly found in "X6" flats soon after window breakage. XPS effluents are low in every flat. After window breakage, it appears that the apartment furniture ignites and the flow at the window changes: the incoming flow from the façade fire reduces while the out-coming flow from the apartment increases with the apartment fire intensity. Thus, the contribution from exterior effluents reduces with time after window breakage. The effluents from the furniture are then dominant. The effluents from the façade elements are mainly found in the "X6" flats because they are contained inside the initial vertical fire plume.

For comparison purposes, the relative influences of the main contributors to the toxic gas FED for gas yield scenario 6 are indicated in Figure 17.

However, for each scenario investigated, the furniture contribution is dominant a few minutes after window breakage, when the apartment contents ignite. The contributions from the XPS and the window reveal insulant appear to be negligible in all scenarios.

The cumulative contribution of the combustion products from the different materials, as a function of time, for the gas yield scenarios 1 and 6, are shown in Figure 18, for the kitchen of flat 196. The change in conditions, and thus contributions from the effluents, and in particular for the façade insulant and the apartment furniture, is clearly visible. In the few minutes just after the window breakage, effluents from the apartment furniture, and the PE and PVC used in the building fabric, are dominant. This is shown in Figure 19 where the contribution to FED for the effluents is illustrated at the time to FED = 0.1, FED = 0.5 and FED = 1 for scenarios 1 and 6 applied to the kitchen of Flat 196.

The contribution of the apartment furniture is already contained inside the plume due to lower flat fires. When the kitchen content ignites approximately 5 min after the window breakage, its contribution increases and those of the PIR façade insulant decrease when the incoming flow from the exterior reduces.

6 | INVESTIGATION INTO CHANGING THE INSULATION MATERIAL

The impact of using non-combustible facade insulation was investigated using the numerical model. The impact of using mineral wool [MW], instead of the PIR that was actually used on Grenfell Tower, was considered in previous studies.[7,8,12,13] The cladding remained as ACM-PE. The modelled fire with an MW insulation shows the same shape as the observations made during the Grenfell fire during the initial vertical fire spread and during the horizontal propagation. The effluents released in each apartment inside the Tower were evaluated for the model using a PIR façade insulant described in the previous sections. The influence of changing the insulation material was investigated by comparing the flows into and out of Flat 26 with those

TABLE 13 Time at which tenability became compromised for the first criterion (thermal or toxic) evaluated numerically at 1.5 m high in the center of the kitchen and of the living room of the Flats 26, 96 and 196—Toxic gas and thermal models #1 and #2—Gas yield scenarios 1 to 9

Flat/level	Location	Window failure time (a.m.)	Under ventilation (a.m.)	Gas yield scenario	Time at which tenability became compromised for the first criterion—thermal/toxic gas model #1 (a.m.)	Time at which tenability became compromised for the first criterion—thermal/toxic gas model #2 (a.m.)
Flat 26—Floor 5	Kitchen	01:18:00	01:32:00	1	01:33:00 (thermal)	01:34:00 (toxic)
				2		01:36:00 (toxic)
				3		01:39:00 (thermal)
				4		01:33:00 (toxic)
				5		01:34:00 (toxic)
				6		01:36:00 (toxic)
				7		01:39:00 (thermal)
				8		01:37:00 (toxic)
				9		01:38:00 (thermal)
	Living room	01:32:00	02:16:00	1 to 9	02:25:00 (thermal)	02:15:00 (thermal)
Flat 96—Floor 12	Kitchen	01:25:00	01:41:00	1	01:47:00 (toxic)	01:43:00 (toxic)
				2	01:49:00 (toxic)	01:45:00 (toxic)
				3	01:52:00 (toxic)	01:47:00 (toxic)
				4	01:45:00 (toxic)	01:41:00 (toxic)
				5	01:46:00 (toxic)	01:41:00 (toxic)
				6	01:48:00 (toxic)	01:43:00 (toxic)
				7	01:53:00 (thermal)	01:57:00 (thermal)
				8	01:50:00 (toxic)	01:45:00 (toxic)
				9	01:52:00 (toxic)	01:52:00 (thermal)
	Living room	01:26:00	01:40:00	1 to 9	01:38:00 (thermal)	01:41:00 (thermal)
Flat 196—Floor 22	Kitchen	01:29:00	01:42:00	1	01:47:00 (toxic)	01:43:00 (toxic)
				2	01:49:00 (toxic)	01:45:00 (toxic)
				3	01:52:00 (thermal and toxic)	01:48:00 (toxic)
				4	01:47:00 (toxic)	01:43:00 (toxic)
				5	01:48:00 (toxic)	01:44:00 (toxic)
				6	01:51:00 (toxic)	01:46:00 (toxic)
				7	01:52:00 (thermal)	01:47:00 (thermal)
				8	01:51:30 (toxic)	01:46:00 (thermal)
				9	01:52:00 (thermal)	01:54:00 (thermal)
	Living room	01:30:00	01:42:00	1	01:43:00 (thermal)	01:41:00 (toxic)
				2		01:43:00 (toxic)
				3		01:46:00 (thermal)
				4		01:41:00 (toxic)
				5		01:41:00 (toxic)
				6		01:43:00 (toxic)
				7		01:46:00 (thermal)
				8		01:44:00 (toxic)
				9		01:46:00 (thermal)

simulated using the PIR façade insulant (see Figure 20). This also allows the validation of the vitiation of this apartment by studying oxygen concentration. The comparison between the models for the flow through the kitchen window of Flat 26 shows a similar range of values both for incoming and outcoming mass rates. The effects of oxygen depletion (respectively reached at 01:32 and 01:35 a.m.

TABLE 14 Summary of the average, minimum and maximum values of the time (a.m.) to reach a toxic gas FED = 1 for the nine gas yield scenarios investigated using the two toxic models

	Kitchen—Toxic Gas Model #1			Kitchen—Toxic Gas Model #2		
FLAT	AVE	MIN	MAX	AVE	MIN	MAX
26	01:42	01:37	01:58	01:39	01:33	01:56
96	01:52	01:45	02:20	01:49	01:41	02:17
196	01:53	01:47	02:24	01:49	01:43	02:21
	Living room - Toxic Gas Model#1			**Living room - Toxic Gas Model#2**		
FLAT	AVE	MIN	MAX	AVE	MIN	MAX
26	02:31	02:25	02:44	02:28	02:20	02:42
96	01:51	01:45	02:12	01:47	01:42	02:09
196	01:52	01:44	02:18	01:47	01:41	02:15

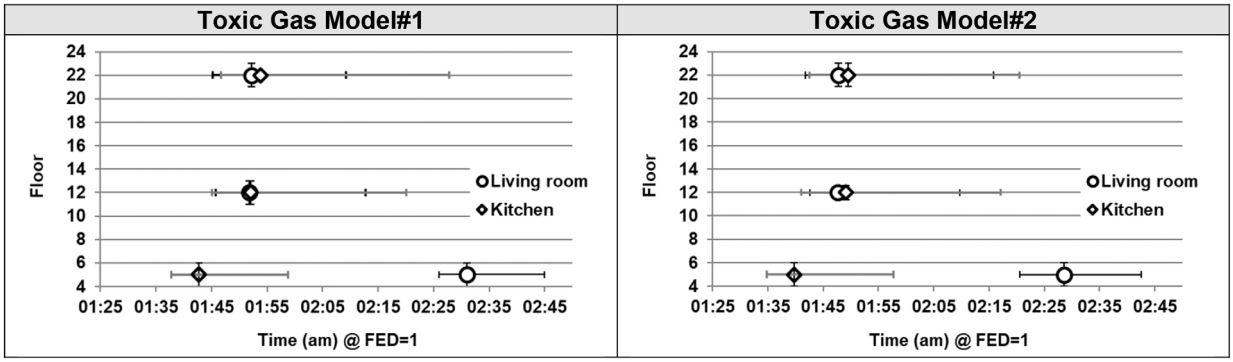

FIGURE 16 Time to reach the toxic gas FED = 1 for the kitchen and living room of Flats 26 (5th floor), 96 (12th floor) and 196 (22nd floor) for the nine gas yield scenarios using the two toxic models

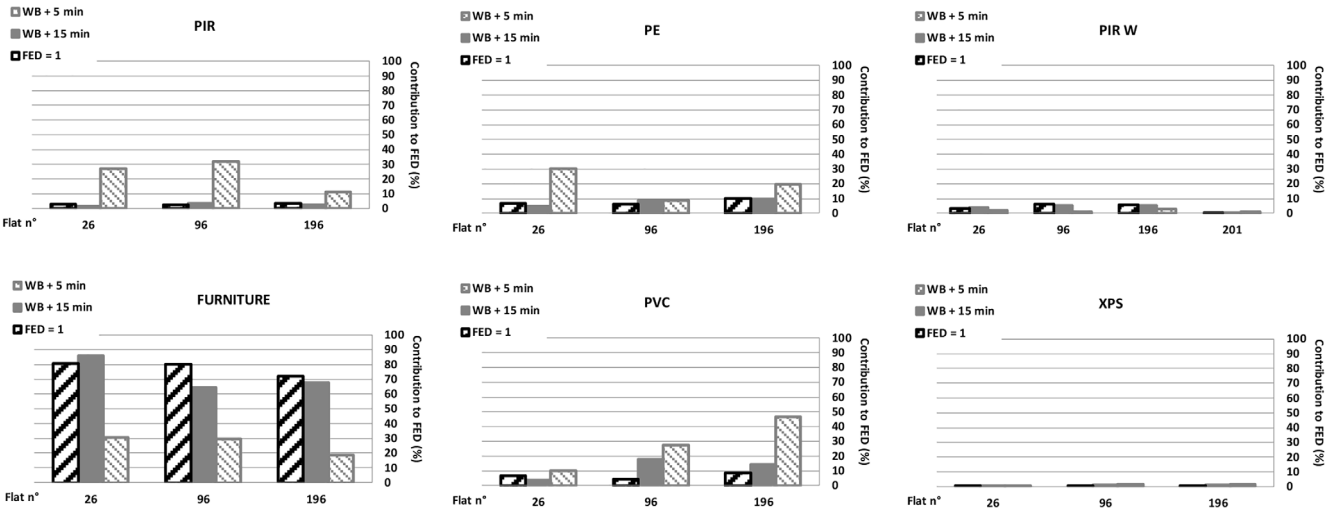

FIGURE 17 Relative contribution of the main elements to the toxic gas FED at the time for FED = 1, at 15 min after window breakage (WB) and at 5 min for the kitchen of Flats 26, 96, 196 and 201—Gas yield scenario 1—Toxic gas model #1

for PIR and MW as observed in Figure 20C)) result in a higher incoming flow through the window as seen in Figure 20A) at 01:35 a.m. for the PIR façade insulant, and 01:37 a.m. for the MW façade insulant.

Species concentrations in Flat 26 and Flat 196 were evaluated numerically at 1.5 m high, in the center of the kitchen and of the living room, for gas yield scenario 1 (Table 9), when MW is used as the façade insulation material. The oxygen concentrations are shown in

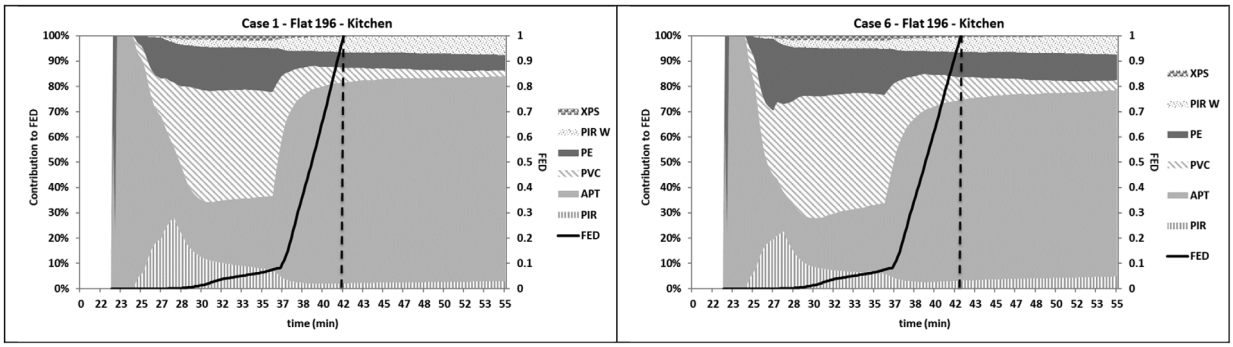

FIGURE 18 Evolution over time of the relative contribution of the main elements to the toxic gas FED—kitchen of Flat 196—gas yield scenarios 1 and 6—Toxic gas model #1 (time to toxic FED = 1 is highlighted with a dashed black line and toxic FED is indicated with solid black line)

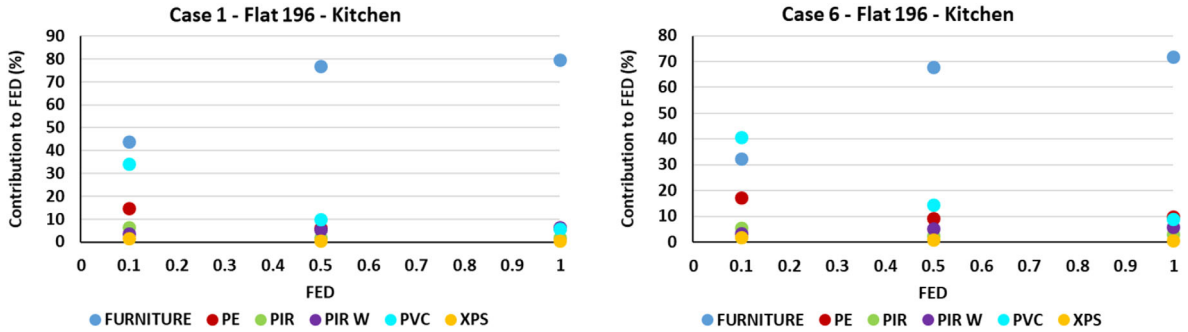

FIGURE 19 Contribution to FED for the effluents is illustrated at the time to FED = 0.1, FED = 0.5 and FED = 1 for Scenarios 1 and 6 applied to the kitchen of Flat 196

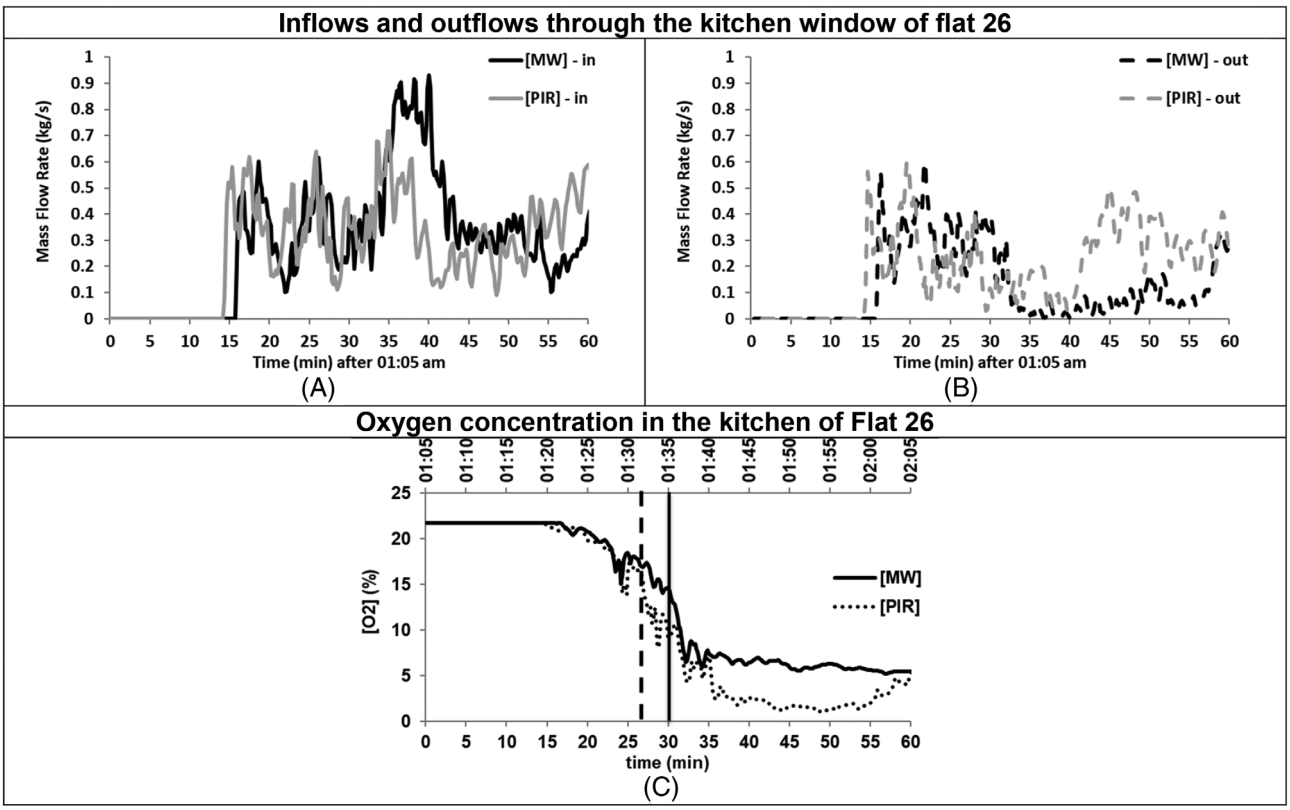

FIGURE 20 Global models of the fire propagation from Flat 16 to Flat 26 to evaluate the accuracy of the inflows and outflows, and the oxygen concentration when [PIR] and [MW] are used as façade insulation materials—the time of oxygen depletion (15%) is marked with a vertical black line in the bottom graph

Figure 21. Under-ventilation occurs in the kitchen and living room of Flats 26 and 196 as indicated in Table 15.

Figure 22 shows the total concentrations, and those for each source material, of the combustion products present in the kitchen and the living rooms of Flat 26, over time. In the kitchen, the CO is released mainly by the apartment furniture. The HCN is mainly released from the furniture and to a lesser extent by the PIR window reveal insulant. In the living room, the CO and HCN come mainly from the apartment furniture.

Similar observations are made for Flat 196 (Figure 22). In the kitchen, the CO is released mainly by the apartment furniture. The HCN is very low and is mainly released from the PIR reveal insulant. In the living room, the CO is released mainly by the apartment furniture. The maximum concentrations of CO are lower than those evaluated when PIR is used as the façade insulant, but they are comparable in order of magnitude, in the range of 6000-8000 μl/L. However, the maximum values are reached faster for an MW façade insulant than PIR. This may be due to the quicker fire spread yielded by the model when MW is used as the façade insulant, as detailed in reference 13.

FEDs and FECs were calculated for the kitchen and living room of Flats 26 and 196 using toxic gas models #1 and #2. By way of example, the toxic gas FED calculation for the kitchen of Flat 26 is shown in Figure 23 for both toxic gas models. Thermal FEDs, according to thermal models #1 and #2, are also indicated.

The times at which tenability became compromised for the first criterion (thermal or toxic) are shown in Table 16. Relative differences between 1 and 8 min are observed between models #1 and #2. The first criterion reached (thermal or toxic) is the same for both rooms in Flat 26, but for flat 196 the first criterion reached depends on the model used.

However, for each apartment investigated, for both models (#1 or #2) used, and regardless of which criteria (thermal or toxic) first caused the loss of tenability, the dominant contribution to FEDs and FECs comes from the apartment furniture when involved in the fire.

A comparison of the estimated times at which tenability became compromised for the first criterion (thermal or toxic) for Flats 26 and 196 when PIR and MW are used as the façade insulant is given in Figure 24 for the gas yield scenario 1. Tenability is lost from the same

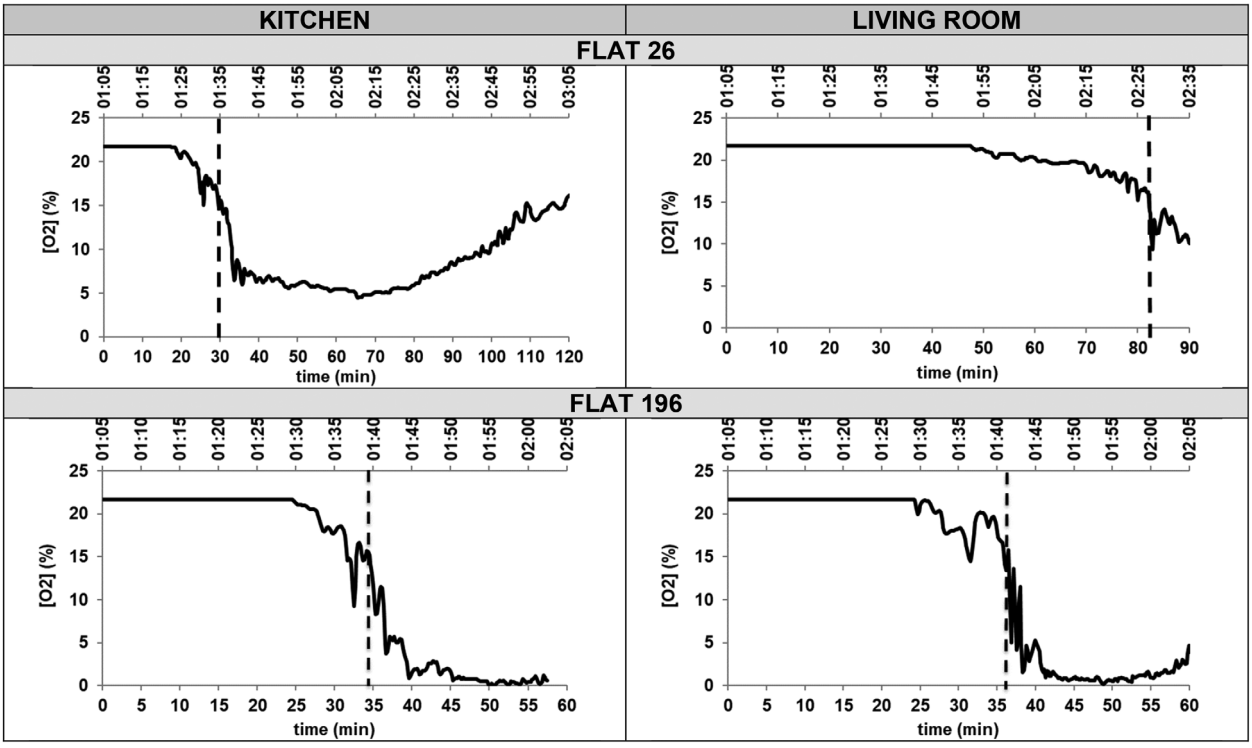

FIGURE 21 Oxygen concentrations evaluated numerically at 1.5 m high in the center of the kitchen and of the living room of Flats 26 and196 when [MW] is used as façade insulation material

TABLE 15 Calculated timing of under-ventilated conditions in Flats 26 and 196 when [MW] is used as the façade insulation material

	Flat 26		Flat 196	
Timescale	**Kitchen**	**Living room**	**Kitchen**	**Living room**
Window failure	01:20 a.m.	01:52 a.m.	01:27 a.m.	01:27 a.m.
Under-ventilation	01:35 a.m.	02:27 a.m.	01:39 a.m.	01:41 a.m.
Relative delay	15 min	35 min	12 min	14 min

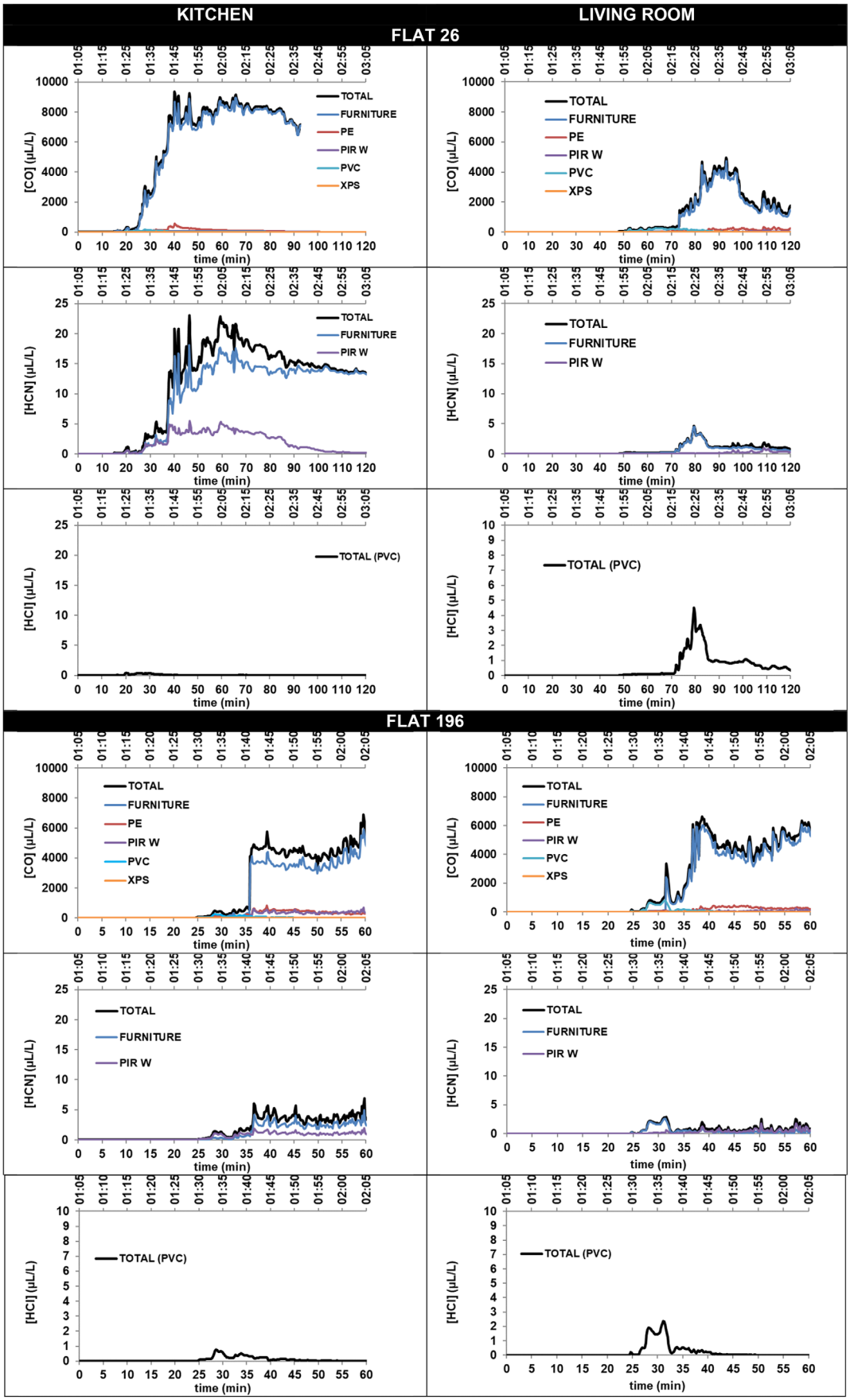

FIGURE 22 Species concentrations and main contributors in the kitchen and living room of Flats 26 and 196 when MW is used as the facade insulation material—Gas yield scenario 1

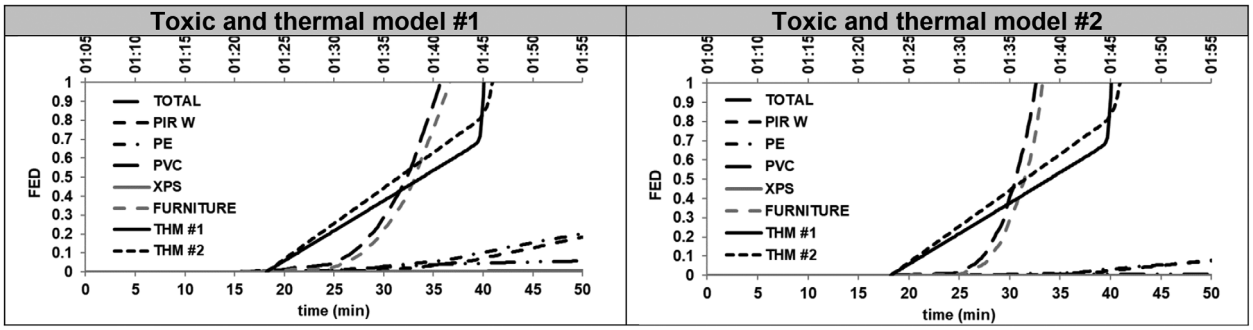

FIGURE 23 Example of FED evaluated numerically at 1.5 m high in the center of the kitchen of Flat 26 when MW is used as the facade insulant following the two tested models—Gas yield scenario 1

TABLE 16 Time at which tenability became compromised for the first criterion—estimated from conditions in Flats 26 and 196 when MW is used as the façade insulant—Gas yield scenario 1

Time at which tenability became compromised for the first criterion (expressed in time)	Flat 26		Flat 196	
	Kitchen	Living room	Kitchen	Living room
Model #1	01:41:00 (toxic criterion)	01:57:00 (thermal criterion)	01:46:00 (thermal criterion)	01:42:00 (thermal criterion)
Model #2	01:38:00 (toxic criterion)	02:05:00 (thermal criterion)	01:43:00 (toxic criterion)	01:43:00 (toxic criterion)

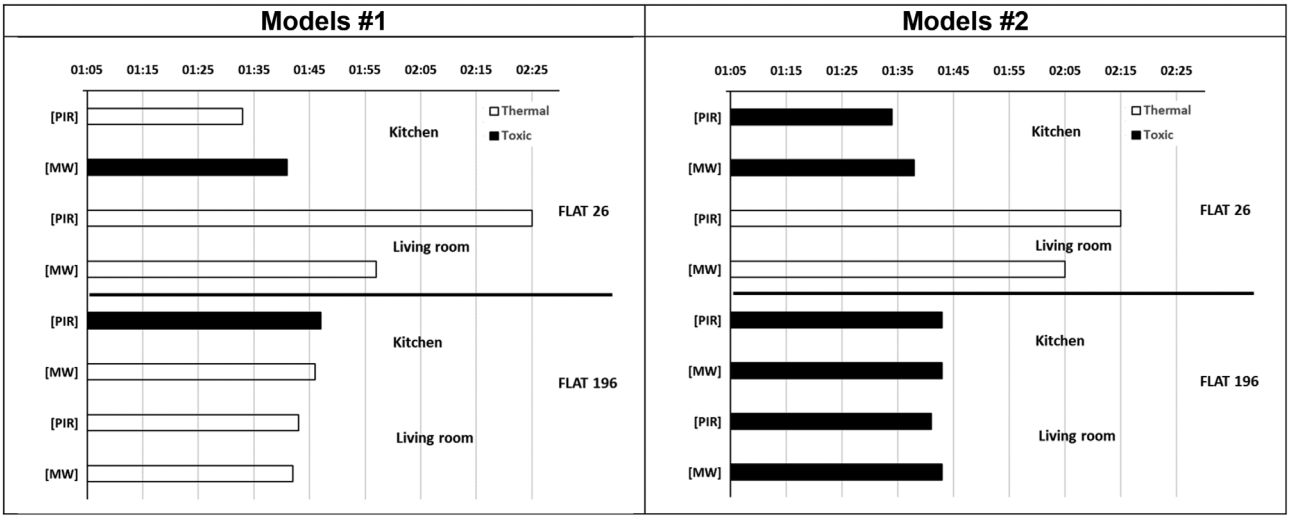

FIGURE 24 Summary of the times at which tenability became compromised in Flats 26 and 196 and the cause of loss of tenability when PIR and MW are used as the façade insulant—Gas yield scenario 1

effect (toxic or thermal) in each room except for the kitchens of Flat 26 and 196 evaluated with model #1. Toxicity dominates for the kitchen of Flat 26 when MW is used as the façade insulant while thermal effects are dominant when PIR is used. On the contrary, in Flat 196, thermal effects are dominant when MW is used while toxicity is dominant when PIR is used and evaluated with the model #1. However, in each room of each flat, loss of tenability is estimated at similar times for both insulant materials. A slight difference of 20 min (Model #1) and 10 min (Model #2) is observed in the living room of Flat 26 where tenability is lost earlier when MW is used. This may be due to the predicted quicker fire spread over the façade with MW that leads to the quicker enhancement of horizontal fire spread. Thus, the façade of the living room of Flat 26 is involved in the fire earlier than in the case with PIR.

7 | CONCLUSIONS

This study comprises a tenability analysis for three different flats in Grenfell Tower, located in the first corner of the Tower that caught fire. An impact model that includes fire loads and fire propagation in the apartments was used to assess tenability conditions inside the Tower. This analysis was conducted in accordance with ISO 13571 (model #1), and using an alternative model adapted to pass/fail analysis (model #2). An extensive bibliographic study was conducted to investigate the CO and HCN yields used in the model to calculate the effects of smoke toxicity. Different hypotheses of gas yields are tested to assess variability and unknowns in the burning conditions. This allowed the quantification of conditions inside the Tower by an analysis of the toxicity conditions due to emissions from either the façade insulant or the apartments' contents. Nine scenarios, based on façade insulant and apartment furniture gas yield assumptions, were evaluated.

For the three flats studied as examples, the mass flow rate into and out of the given kitchen and living room windows was evaluated numerically. For all flats investigated, a change in the flow direction through the windows was observed. Initially, the global flow through the window comes mainly from the exterior plume into the apartment. This is due to the air entrainment from the large flow velocity behind the window from the fully developed façade fire leading to inward flow at the point of window failure. Then, when the fire ignites in the flat, the incoming flow almost stops and the outgoing flow from the apartment to the exterior increases with fire intensity and pressure increase in the compartment.

The local concentration of every species released was evaluated numerically in the kitchen and in the living room of each flat at a height of 1.5 m, corresponding to the position of a human nose, mouth and eyes. The evaluation of flow through windows led to the quantification, in given apartments, of toxic species due to the combustion of either façade materials or the apartment's contents.

The cumulative contribution of the main effluents released as a function of time, for gas yield scenarios 1 and 6 shows the change in conditions, and thus contributions of the effluents from the façade insulant and apartment furniture, and in particular for higher floors. Just after window breakage, effluents from the apartment furniture, and the PE and PVC used in the building fabric, are dominant. Some contribution of the apartment furniture is already contained inside the plume due to lower flat fires. When the kitchen content ignites, a few minutes after the window breakage, its contribution increases, and those of the PIR façade insulant decrease when the incoming flow from the exterior reduces.

For both model #1 and for model #2, and for the majority of the three apartment locations and the nine gas yield scenarios investigated, oxygen depletion is reached first, or at a similar time to the thermal FED, due to the ignition of apartment contents.

Tenability is compromised because of thermal effects before the effects of gas toxicity for the majority of the scenarios and locations inside the apartments. For the 54 cases investigated, 40 occurrences of thermal criteria reached the first appearance, and thus represent 75% of the investigated scenarios. However, smoke propagation from the fire-impacted apartments to the rest of the structure may increase the impact of gas toxicity and reduce that of thermal effects as smoke is cooled down and diluted with distance from the apartments. This justifies a deeper analysis of smoke toxicity sources. The main contribution to gas toxicity comes from the apartment furniture in every scenario and location, once the window has failed.

The impact of using a non-combustible façade insulant was also investigated using the numerical model. A model was created with MW instead of the PIR façade insulation while the cladding remained as ACM-PE. The modelled fire with MW insulation showed the same shape as the observations made during the Grenfell disaster. The effluents released in each apartment inside the Tower were evaluated for the model incorporating a PIR façade insulant. The influence of changing the insulation material was investigated by comparing the flows into and out of Flat 26 with those simulated using the model with a PIR façade insulant. This also allowed the validation of the vitiation of this apartment by studying oxygen concentration. The comparison between the models for the flow through the kitchen window of Flat 26 showed a similar range of values both for incoming and outgoing mass flow rates. The maximum concentrations of CO are lower than those evaluated when PIR is used as façade insulant, but they are comparable in order of magnitude, in the range of 6000-8000 μl/L. However, the maximum values are reached faster for an MW façade insulant than PIR. This may be due to the quicker fire spread yield by the model when MW is used as the façade insulant.

The comparison of estimated times at which tenability became compromised for the first criterion (thermal or toxic) for Flats 26 and 196 when PIR and MW are used as the façade insulant showed that, in both cases, tenability is lost because of the same effect (toxic or thermal) in each room except for the kitchens of Flats 26 and 196 evaluated with the Model #1. Toxicity dominates in Flat 26 when MW is used as the façade insulant, while thermal effects are dominant when PIR is used. On the contrary, in Flat 196, thermal effects are dominant when MW is used while toxicity is dominant when PIR is used. However, in each room of each Flat, loss of tenability is estimated at similar times for both insulant materials. A slight difference of 20 min (Model #1) and 10 min (Model #2) is observed in the living room of Flat 26 where tenability is lost earlier when MW is used. This may be due to the predicted quicker fire spread over the façade with MW that leads to the quicker enhancement of horizontal fire spread. Thus, the façade of the living room of Flat 26 is involved in the fire earlier than in the case with PIR. The thermal effects and toxicity are due to the ignition of the apartment contents.

The main results of the present paper showed that the same conclusion can be made regardless of the input data for toxicity and the model used, within the limits of the studied dataset and conditions. Fires from the apartments quickly drive tenability conditions, independently of the dataset and model used, and even if MW is used instead of PIR as façade insulant.

Even if the numerical model addressed in this paper correlates well with the observations during the Grenfell Tower fire, several modelling assumptions were needed and constitute limitations of the model. As discussed in,[10,12] the numerical hypothesis must be considered for the model developed for the accurate fine grid to be

applied to a coarser one as used in the present model. Furthermore, the CFD code FDS used in this study considers constant effluent yields for a given combustion reaction, and these yields will not depend on the ventilation conditions. The main scenarios addressed in the toxicity analysis were based on an extensive literature review to investigate the toxic and asphyxiant effluent yields, to be used in calculations. The objective was to reproduce in the simulations the variation in the CO and HCN yields depending on the fire development. The sensitivity analysis and uncertainty calculations of such work are very complex and will be included in further parts of the study.

The analysis of tenability conditions inside Grenfell Tower showed that the same conclusion can be made regardless of the input data for toxic gas yields and the model used, within the limits of the studied dataset and conditions. The overall conclusion is that fires involving furnishings in the apartments quickly drive tenability conditions, independently of the dataset and model used, and even if MW is used instead of PIR as a façade insulant.

Further steps of this research will be dedicated to the tenability evaluation in the lobbies and stairs of the Tower. Additional research will focus on the sensitivity analysis of all the previous steps of the reconstruction.

ACKNOWLEDGEMENTS

This reconstruction only uses publicly available Grenfell Tower Inquiry data or data published in the scientific literature. This work has been partially financed by Kingspan. The sponsor has not been involved in the results nor the conclusions of this paper.

ORCID

Eric Guillaume https://orcid.org/0000-0002-3055-2741
Virginie Dréan https://orcid.org/0000-0002-3216-1808
Bertrand Girardin https://orcid.org/0000-0003-2206-9626
Talal Fateh https://orcid.org/0000-0002-4204-0540

REFERENCES

1. Moore-Bick M. (2019) *Grenfell Tower Inquiry: Phase 1 Report - Report of the Public Inquiry into the Fire at Grenfell Tower on June 14, 2017*, October 2019.
2. Bisby L., Grenfell Tower Inquiry. Phase 1—Final report. Dated 21st October 2018. https://www.grenfelltowerinquiry.org.uk/evidence/professor-luke-bisbys-expert-report-supplemental
3. Lane B., Grenfell Tower- fire safety investigation: The fire protection measures in place on the night of the fire, and conclusions as to: the extent to which they failed to control the spread of fire and smoke; the extent to which they contributed to the speed at which the fire spread. Dated October 24, 2018, https://www.grenfelltowerinquiry.org.uk/evidence/dr-barbara-lanes-expert-report-supplemental
4. Torero, J., Grenfell Tower: Phase 1 report. TAEC Ref GFT-1710-0C-001-PR-01. 23rd May 2018, revised 21st October 2018, https://www.grenfelltowerinquiry.org.uk/evidence/professor-jose-l-toreros-expert-report-supplemental
5. Professor David Purser's expert report, Phase 1, Dated: 5th November 2018, https://www.grenfelltowerinquiry.org.uk/evidence/professor-david-pursers-expert-report
6. Guillaume E, Dréan V, Girardin B, Benameur F, Fateh T. Reconstruction of Grenfell tower fire—part 1: lessons from observations and determination of work hypotheses. 2019;44:3-14. doi:10.1002/fam.2766
7. Dréan V, Girardin B, Guillaume E, Fateh T. Numerical simulation of the fire behaviour of Façade equipped with aluminium composite material-based claddings—model validation at intermediate-scale. *Fire Mater*. 2019;2019:1-18. doi:10.1002/fam.2745
8. Dréan V, Girardin B, Guillaume E, Fateh T. Numerical simulation of the fire behaviour of Façade equipped with aluminium composite material-based claddings—model validation at large scale. *Fire Mater*. 2019;2019:1-18. doi:10.1002/fam.2759
9. Guillaume E, Fateh T, Schillinger R, Chiva R, Ukleja S. Study of fire behaviour of façade mock-ups equipped with aluminium composite material-based claddings using intermediate-scale test method. *Fire Mater*. 2018;2018:1-17. doi:10.1002/fam.2635
10. Guillaume E, Dréan V, Girardin B, Koohkan M, Fateh T. Reconstruction of Grenfell tower fire—part 2: a numerical investigation of the fire propagation and behaviour from the initial apartment to the Grenfell Tower Façade. *Fire Mater*. 2019;44(1):15-34. doi:10.1002/fam.2765
11. Koohkan M, Dréan V, Guillaume E, Girardin B, Fateh T, Duponchel X. Reconstruction of Grenfell tower fire - Thermomechanical analysis of window failure during the Grenfell Tower disaster. *Fire Technol*. 2020;57:69-100. doi:10.1007/s10694-020-00980-4
12. Guillaume E, Dréan V, Girardin B, Benameur F, Koohkan M, Fateh T. Reconstruction of Grenfell tower fire—part 3: numerical simulation of the Grenfell Tower disaster: contribution to the understanding of the fire propagation and behaviour during the vertical fire spread. *Fire Mater*. 2019;44(1):35-57. doi:10.1002/fam.2763
13. Guillaume E, Dréan V, Girardin B, Fateh T. Reconstruction of Grenfell tower fire—part 4: contribution to the understanding of the fire propagation and behaviour during the horizontal fire spread. *Fire Mater*. 2020;44(8):1072-1098. doi:10.1002/fam.2911
14. McGrattan K, Hostikka S, McDermott R, Floyd J, Weinschenk C, Overholt K. FDS fire dynamics simulator (version 6.7.1) User's guide. *NIST Special Publication 1019*. 2019. doi:10.6028/NIST.SP.1019
15. McGrattan K., Hostikka S., McDermott R., Floyd J., Weinschenk C., Overholt K. (2019). FDS Fire Dynamics Simulator (Version 6.7.1) Technical Reference Guide Volume 1: Mathematical Model, NIST Special Publication 1018-1, 10.6028/NIST.SP.1018
16. McGrattan K., Hostikka S., McDermott R., Floyd J., Weinschenk C., Overholt K. (2019). FDS Fire Dynamics Simulator (Version 6.7.1) Technical Reference Guide Volume 2: Verification, NIST Special Publication 1018-2, February 4, 2019, 10.6028/NIST.SP.1018
17. McGrattan K., Hostikka S., McDermott R., Floyd J., Weinschenk C., Overholt K. (2019). FDS Fire Dynamics Simulator (Version 6.7.1) Technical Reference Guide Volume 3: Validation, NIST Special Publication 1018-3, February 4, 2019, 10.6028/NIST.SP.1018
18. Guillaume E, Didieux F, Thiry A, Bellivier A. Real-scale fire tests of one bedroom apartments with regard to tenability assessment. *Fire Saf J*. 2014;70:81-97. doi:10.1016/j.firesaf.2014.08.014
19. Purser DA. Toxic combustion product yields as a function of equivalence ratio and flame retardants in under-ventilated fires: bench-large-scale comparisons. *Polymers*. 2016;8:330. doi:10.3390/polym8090330
20. Babrauskas V, Harris RH, Braun E, Levin BC, Paabo M, Gann RG. *The Role of Bench-Scale Test Data in Assessing Real-Scale Fire Toxicity, Technical Note 1284*. Gaithersburg, MD: National Bureau of Standards and Technology; 1991.
21. Marsh ND, Gann RG. *Smoke component yields from bench-scale fire tests: 4. Comparison with Room Fire Results, NIST Technical Note 1763*. Gaithersburg, MD: National Institute of Standards and Technology; 2013.
22. Forell B, Hosser D. The relationship between ventilation conditions and carbon monoxide source term in fully-developed compartment fires. *Proceedings of the 5th International Seminar on Fire and Explosion Hazards*. Edinburgh, UK; 2007:23-27.
23. Marquis DM, Hermouet F, Guillaume E. Effects of reduced oxygen environment on the reaction to fire of a poly(urethane-isocyanurate) foam. *Fire Mater*. 2016;41(3):245-274. doi:10.1002/fam.2378

24. Pitts, W.M. (1995). The global equivalence ratio concept and the formation mechanisms of carbon monoxide in enclosure fires, Prog, *Energy Combust Sci* Vol. 21, pp. 197-23719,95
25. Cuesta A, Abreu O, Alvear D. *Evacuation Modeling Trends*. Springer; 2016. doi:10.1007/978-3-319-20708-7
26. Stec AA, Hull TR. Assessment of the fire toxicity of building insulation materials. *Energ Build*. 2011;43:498-506.
27. Kaczorek K, Stec AA, Hull TR. Carbon monoxide generation in fires: effect of temperature on halogenated and aromatic fuels. *Fire Saf Sci*. 2011;10:253-263.
28. Stec AA, Hull TR, Lebek K, Purser JA, Purser DA. The effect of temperature and ventilation condition on the toxic product yields from burning polymers. *Fire Mater Int J*. 2008;32(1):49-60.
29. Purser JA, Purser DA, Stec AA, et al. Repeatability and reproducibility of the ISO/TS 19700 steady state tube furnace. *Fire Saf J*. 2013;55: 22-34.
30. Crewe RJ, Lyons AG, Hull TR, Stec AA. Asphyxiant yields from common polymers in under-ventilated fires in the large instrumented fire enclosure (LIFE). *Fire Saf J*. 2017;91:982-988.
31. Purser DA, Purser JA. HCN yields and fate of fuel nitrogen for materials under different combustion conditions in the ISO 19700 tube furnace and large-scale fires. *Fire Saf Sci*. 2008;9: 1117-1128.
32. ISO/TR 20118:2019 Plastics—Guidance on fire characteristics and fire performance of PVC materials used in building applications, April 2019
33. McKenna ST, Hull TR. The fire toxicity of polyurethane foams. *Fire Sci Rev*. 2016;5(1):3.
34. ISO 13571:2012 Life-threatening components of fire—Guidelines for the estimation of time to compromised tenability in fires
35. ISO/TR 13571–2:2016 Life-threatening components of fire—Part 2: Methodology and examples of tenability assessment
36. Project ISO/DIS 13571–1. Life-threatening components of fire Part 1: Guidelines for the estimation of time to compromised tenability in fires. Public draft, accessed June 2020.
37. Pauluhn J. Estimation of time to compromised tenability in fires: is it time to change paradigms? *Regul Toxicol Pharmacol*. 2020;111: 104582. doi:10.1016/j.yrtph.2020.104582
38. Purser DA. Toxicity assessment of combustion products. In: DiNenno PJ, ed. *SFPE Handbook of Fire Protection Engineering*. 4th ed. Quincy, MA: NFPA; 2008 pp II-96-II-193, 2008.
39. Wieczoreck CJ, Dembsey NA. Human variability correction factors for use with simplified engineering tools for predicting pain and second degree skin burns. *J Fire Protect Eng*. 2001;11(2):88-111.
40. Kaplan HL, Grand AF, Switzer WG, Mitchell DS, Rogers WR, Hartzell GE. Effects of combustion gases on escape performance of the baboon and the rat. *J Fire Sci*. 1985;3(4):228-244.
41. Specified Level of Toxicity (SLOT) and Significant Likelihood of Death (SLOD). http://www.hse.gov.uk/chemicals/haztox.htm (accessed: April 2020).
42. Guillaume E. (2006). Effets du feu sur les personnes—Synthèse bibliographique. LNE Report Nr G020284/C672X01/CEMATE/1, http://www.lne.fr/publications/guides-documents-techniques/rapport-effets-feu-personnes-eric-guillaume.pdf
43. Guillaume E.(2012). Toxicité des fumées d'incendie; SE 2 060, Technique de l'Ingénieur, traité sécurité, 2012.
44. *Acute Exposure Guideline Levels for Selected Airborne Chemicals, Vol. 11*. National Research Council, National Academies Press; 2012:167-256 ISBN-13: 978-0-309-25481-6.
45. ECETOC Technical report No. 110. Guidance on Assessment Factors to Derive a DNEL (October Published 2010).
46. ECETOC Technical report No. 86. Derivation of Assessment Factors for Human Health Risk Assessment (Published February 2003).
47. European Commission. REACH TGD: Technical Guidance Document on Risk Assessment in support of Commission Directive 93/67/EEC on Risk Assessment for new notified substances, Commission Regulation (EC) No 1488/94 on Risk Assessment for existing substances, Directive 98/8/EC of the European Parliament and of the Council concerning the placing of biocidal products on the market. https://echa.europa.eu/documents/10162/16960216/tgdpart1_2ed_en.pdf (accessed: April 2020).
48. Standing Operating Procedures for Developing Acute Exposure Guideline Levels for Hazardous Chemicals. Subcommittee on acute exposure guideline levels committee on toxicology—board on environmental studies and toxicology, Commission on Life Sciences. National Research Council, National Academies Press, 2012, ISBN 0-309-07553–X.
49. ISO/TR 20118:2019 Plastics—Guidance on fire characteristics and fire performance of PVC materials used in building applications.
50. Luche J, Rogaume T, Guillaume E. Characterization of polyvinyl chloride–based floor covering thermal decomposition parameters in a cone calorimeter. *J Fire Sci*. 2020;38(5):433-461. doi:10.1177/0734904120944340

How to cite this article: Guillaume E, Dréan V, Girardin B, Fateh T. Reconstruction of the Grenfell Tower fire—Part 5: Contribution to the understanding of the tenability conditions inside the apartments following the façade fire. *Fire and Materials*. 2022;1-28. doi:10.1002/fam.3054